DAMPING REDUCTION EQUATION FOR THE EQUIVALENT LINEAR ANALYSIS OF SEISMIC ISOLATED STRUCTURES SUBJECTED TO NEAR FAULT GROUND MOTIONS

A THESIS SUBMITTED TO
THE GRADUATE SCHOOL OF NATURAL AND APPLIED SCIENCES
OF
MIDDLE EAST TECHNICAL UNIVERSITY

BY

EMRAH KARA

IN PARTIAL FULFILLMENT OF THE REQUIREMENTS
FOR
THE DEGREE OF MASTER OF SCIENCE
IN
EARTHQUAKE STUDIES

JUNE 2019

Approval of the thesis:

DAMPING REDUCTION EQUATION FOR THE EQUIVALENT LINEAR ANALYSIS OF SEISMIC ISOLATED STRUCTURES SUBJECTED TO NEAR FAULT GROUND MOTIONS

submitted by **EMRAH KARA** in partial fulfillment of the requirements for the degree of **Master of Science in Earthquake Studies Department, Middle East Technical University** by,

Prof. Dr. Halil Kalıpçılar
Dean, Graduate School of **Natural and Applied Sciences** _____

Prof. Dr. Ayşegül Askan Gündoğan
Head of Department, **Earthquake Studies** _____

Prof. Dr. Murat Dicleli
Supervisor, **Earthquake Studies, METU** _____

Prof. Dr. Ayşegül Askan Gündoğan
Co-Supervisor, **Earthquake Studies, METU** _____

Examining Committee Members:

Prof. Dr. Uğurhan Akyüz
Earthquake Studies, METU _____

Prof. Dr. Murat Dicleli
Earthquake Studies, METU _____

Prof. Dr. Ayşegül Askan Gündoğan
Earthquake Studies, METU _____

Assoc. Prof. Dr. Ferhat Akgül
Engineering Sciences, METU _____

Prof. Dr. Tolga Akış
Civil Engineering, Atılım University _____

Date: 25.06.2019

I hereby declare that all information in this document has been obtained and presented in accordance with academic rules and ethical conduct. I also declare that, as required by these rules and conduct, I have fully cited and referenced all material and results that are not original to this work.

Name, Surname: Emrah Kara

Signature:

ABSTRACT

DAMPING REDUCTION EQUATION FOR THE EQUIVALENT LINEAR ANALYSIS OF SEISMIC ISOLATED STRUCTURES SUBJECTED TO NEAR FAULT GROUND MOTIONS

Kara, Emrah
Master of Science, Earthquake Studies
Supervisor: Prof. Dr. Murat Dicleli
Co-Supervisor: Prof. Dr. Ayşegül Askan Gündoğan

June 2019, 69 pages

In this study, a new damping reduction equation is proposed to obtain reasonable estimates of the actual nonlinear responses of seismic isolated structures (SIS) subjected to near fault ground motions (NGM) with forward-rupture-directivity effect, using equivalent linear analysis (ELA) procedure. For this purpose, first, a set of 29 NGM are selected and grouped according to their site soil classification. Then, the average response spectra of the NGM are plotted and a smoothed design response spectrum for each set of ground motions are obtained. Next, nonlinear time history analysis (NLTHA) and ELA of SIS are performed for the selected ground motions. Subsequently, the average of the isolator displacements calculated from the NLTHA are obtained for each set of NGM considered in the analyses. Then, the damping reduction factor required to obtain an isolator displacement equal to the average isolator displacements obtained from the NLTHA of SIS is back calculated via the ELA procedure. Next, the variation of the damping reduction factor is plotted as a function of various combinations of the parameters considered in this research in dimensionless form and nonlinear regression analyses are performed to formulate the damping reduction equation. The isolator characteristic strength, post elastic period, the corner period of the response spectrum and peak ground acceleration are found to

affect the damping reduction factor and hence, the displacements obtained from ELA. The proposed damping reduction equation is found to yield more reasonable estimates of the actual nonlinear responses compared to those available in the literature and design codes.

Keywords: Near Fault Ground Motions, Seismic Isolation, Equivalent Linear Analysis, Damping Reduction Equation

ÖZ

YAKIN SAHA DEPREM ETKİSİNE MARUZ KALAN SİSMİK İZOLATÖRLÜ YAPILARIN EŞDEĞER DOĞRUSAL ANALİZİ İÇİN ENERJİ SÖNÜMLEME DENKLEMİ

Kara, Emrah
Yüksek Lisans, Deprem Çalışmaları
Tez Danışmanı: Prof. Dr. Murat Dicleli
Ortak Tez Danışmanı: Prof. Dr. Ayşegül Askan Gündoğan

Haziran 2019, 69 sayfa

Bu çalışmada, ileri yönelim etkili yakın saha depremlere (YSD) maruz kalan sismik izolatörlü yapıların (SİY) doğrusal olmayan davranışlarını eşdeğer doğrusal (ED) analiz yöntemi ile daha iyi tahmin edebilmek için yeni bir enerji sönümleme denklemi önerilmiştir. Bu amaçla, ilk olarak 29 YSD seçilmiş ve etki alanı zemin sınıfına göre gruplandırılmıştır. Sonra YSD'nin ortalama davranış spektrumları çizilmiş ve her bir deprem seti için işlenmiş tasarım davranış spektrumları elde edilmiştir. Daha sonra seçilmiş deprem kayıtları ile sismik izolatörlü yapıların zaman tanım alanında hesap yöntemi (ZTAHY) ve ED analizleri yapılmıştır. Bundan sonra, bu analizlerde kullanılan her bir set için YSD ile yapılan ZTAHY analizlerinden elde edilen deplasmanların ortalamaları hesaplanmıştır. Ortalama deplasmanları ED analizler ile elde etmek için gerekli enerji sönümleme katsayıları, ED analizini geriye doğru hesaplayarak elde edilmiştir. Bu enerji sönümleme katsayılarının, bu çalışmada kullanılan parametrelerin boyutsuz halleri ile davranışı incelenmiş ve doğrusal olmayan regresyon analizi ile enerji sönümleme denklemi formüle edilmiştir. İzolatör akma dayanımı, elastik olmayan titreşim periyodu, davranış spektrumu ikinci köşe periyodu ve en büyük yer ivmesinden etkilendiğini, dolayısı ile ED analiz ile elde edilen deplasman sonuçlarının etkilediği tespit edilmiştir. Son olarak önerilen enerji

sönümleme denklemi kullanılarak yapılan ED analizlerin, doğrusal olmayan gerçek davranışı literatürde ve tasarım kodlarında bulunan enerji sönümleme denklemi kullanılarak yapılan analizlere göre daha yakın tahmin ettiği saptanmıştır.

Anahtar Kelimeler: Yakın Saha Depremleri, Sismik İzolatör, Eşdeğer Doğrusal Analiz, Enerji Sönümleme Denklemi,

To my family

ACKNOWLEDGEMENTS

I would like to express my deepest and sincere gratitude to my supervisor, Prof. Dr. Murat DİCLELİ for his extreme patience, encouragement, understanding and valuable guidance during my graduate study. I would not be able complete this thesis without his student-oriented attitude, forbearance to the confronted issues and also his tolerant guidance. I am very thankful for his great interest and help. Likewise, I am also very thankful to my co-supervisor Prof. Dr. Ayşegül ASKAN GÜNDOĞAN for her guidance.

I am grateful to the generous person, Enes KARAASLAN for his awesome brotherhood. He always boosted my motivation and fostered his support in all challenging stages of this thesis. I also cannot overlook the technical supports of my dear colleague Raşit Emre ÇAKIR and former-manager Zeki HARPUTOĞLU. In addition I would like to thank my former-managers Gülden ÇETİN and Fikret TULUMTAŞ for their patience and supports.

Finally, I would like to thank to my dear family. This thesis is dedicated to them. Without their support, love, patience and belief in me; I would never have accomplished this, hence, I would like to thank to my mother Birgül KARA, my father Hacı KARA and my sister Esra KARA for their love, understanding, toleration and support.

TABLE OF CONTENTS

LIST OF TABLES

TABLES

LIST OF FIGURES

FIGURES

CHAPTER 1

INTRODUCTION

1.1. Introduction

Design specifications such as American Association of State Highway and Transportation Officials Guide specification for seismic Isolation Design (AASHTO 2014), European Standard Anti Seismic Devices (EN 15129 2010), American Society of Civil Engineers Minimum Design Loads and Associated Criteria for Buildings and Other Structures (ASCE 7-16 2016) and National Earthquake Hazards Reduction Program Recommended Seismic Provisions for New Buildings and Other Structures (NEHRP 2009) propose several methods for the analyses of seismic isolated bridges and buildings. These proposed methods are uniform load method, single-mode spectral analyses method, multi-mode spectral analyses method and nonlinear time history analysis (NLTHA) method. Uniform load, single and multi-mode spectral analyses methods require a linear elastic analysis procedure while the NLTHA method requires a nonlinear analysis procedure. Since the behavior of seismic isolated structures is nonlinear in nature, the NLTHA method produces a better estimation of the actual nonlinear responses of such structures. However, NLTHA method requires extensive computational effort and selection of a set of ground motion data appropriate to the design spectrum, site conditions, fault rupture mechanism and distance to the governing fault. Therefore, linear analyses methods are more often preferred in practice for the preliminary and final design of seismic isolated structures. For instance, the design of many seismically isolated hospitals and lifeline bridges in different parts of the World have been performed using linear analyses procedures but verified via NLTHA using actual prototype test data defining the actual characteristics of the seismic isolation bearings (Buckle et al. 2006; Dicleli, 2002; Kubin et al. 2012; Rousis et al. 2003).

As the behavior of seismic isolation systems is inherently nonlinear, to conduct the analysis of seismic isolated structures using linear analysis procedures, equivalent linear properties of the seismic isolation system needs to be defined. These equivalent linear properties are effective stiffness, effective period and effective damping ratio to account for the hysteretic energy dissipation of the isolators. The analyses conducted using such equivalent linear properties is called equivalent linear analysis (ELA). The ELA method involves an iterative procedure where an isolator displacement is assumed. Based on the assumed isolator displacement, the equivalent linear properties of the isolators are calculated to perform linear analysis of the structure. To include the effect of hysteretic damping of the seismic isolation system in the analysis, the 5% damped response spectrum used in the analysis is divided by a damping reduction factor, which is a function of the effective damping ratio and in some cases some additional parameters. This damping reduction factor is defined in design specifications. The ELA of seismic isolated structures using the damping reduction factors proposed in design specifications generally produce reasonably good estimates of the nonlinear responses of such structures subjected to far fault ground motions (Hwang and Sheng 1993; Hwang 1996; Hwang et al. 1997; Franchin et al. 2001). However, for seismic isolated structures subjected to Near Fault Ground Motions (NGM) with Forward Rupture Directivity Effect (FRDE), the ELA method that use the damping reduction factors proposed in design specifications generally underestimates the nonlinear responses of such structures. This is mainly due to the effect of long duration, intense velocity pulses inherent in such ground motions producing very large isolator displacements (Dicleli, 2006, 2007, 2008). Therefore, there is an urgent need for damping reduction factors in design codes specific to the ELA of structures subjected to NGM with FRDE.

1.2. Research Objective, Scope and Assumptions

The main objective of this research study is to develop an effective and simple damping reduction equation for the ELA of seismic isolated structures subjected to NGM with FRDE.

In this study, the damping reduction factors are obtained for ELA of seismic isolated structures subjected to NGM with FRDE. NGM with backward rupture directivity effect are not included in this study. The damping reduction factor used in ELA is obtained by setting the response from ELA equal to that from NLTHA. Both the ELA and NLTHA are performed for seismic isolated structures modeled by a single isolator supporting a rigid mass (superstructure) to decouple the response of the seismic isolated structures from the effect of the superstructure and substructure parameters.

1.3. Thesis Outline

The outline of this research study is as follows:

1- First, a set of 29 NGM with FRDE are obtained from the PEER (Pacific Earthquake Engineering Research) database. These ground motions are grouped according to their soil classifications into a set of namely; A&B, C and D. Soil classifications A and B are considered together due to the lack of NGM data in these soil classifications and thus, include only seven NGM. Other sets of ground motions include 11 NGM. Particular attention is given to the selection of these ground motions such that, their 5% damped elastic response spectra are similar within each soil classification. As the average smoothed spectrum is used in the ELA and compared with the average of the results from the NLTHA, the number of ground motions used in the analyses does not have a meaningful impact on the results of this research study. This has already been confirmed by using 21 rather than 29 NGM where similar results are obtained.

2- Then, the average response spectra of the ground motions used in each set are plotted and a smoothed design response spectrum for each set of ground motions are

obtained using nonlinear minimum least square regression analyses. The average of the velocity pulse periods of the ground motions within each set is used to characterize the smoothed design response spectrum. The smoothed design response spectra are used in the ELA of single degree of freedom structures (an isolator supporting a rigid mass).

3- Next, NLTHA and ELA of single degree of freedom structures are performed for the selected ground motions. The analyses are repeated for an extensive range of parameters including peak ground acceleration, characteristic strength and post-elastic stiffness of the isolator for all the soil types and associated smoothed design response spectra as characterized by the average velocity pulse period from the ground motions within each set. This resulted in 3625 NLTHA and 375 ELA.

4- Subsequently, the average of the isolator displacements calculated from the NLTHA are obtained for each set of ground motions for the site soil classifications considered in the analyses. This produced 375 isolator displacement values for the range of parameters considered in the analyses.

5- Then, the damping reduction factor required to obtain an isolator displacement equal to the average isolator displacements obtained from the NLTHA of the single degree of freedom structure for each set of ground motions is back-calculated via the ELA procedure,

6- Next, the variation of the damping reduction factor is plotted as a function of the various combinations of the parameters considered in this research study in dimensionless form. Then, nonlinear regression analyses are performed to formulate the damping reduction equation as a function of the dimensionless forms of the combination of parameters considered in the analyses.

7- The damping reduction equation obtained in the previous step contains the average velocity pulse period obtained for each set of ground motions. This parameter is not practical to use in the ELA of seismic isolated structures since only the design response spectrum is available to the designer. Consequently, additional studies are

performed to relate the velocity pulse period to the corner period of the design response spectrum at the junction of the equal energy and equal displacement regions. As a result of this additional study, an equation is obtained that relates the velocity pulse period to the corner period of the design spectrum. This relationship is substituted in place of the velocity pulse period to obtain the final simplified form of the damping reduction equation.

8- Next, the proposed damping reduction equation is verified using a different set of NGM for various site soil classifications. In addition, a comparative assessment of the ELA results using the proposed damping reduction equation and those proposed by various researchers and design codes is performed to demonstrate the accuracy of the proposed damping reduction equation compared to those proposed by other researchers and design codes.

1.4. Properties of Typical Seismic Isolators

Seismic isolators are generally categorized as rubber-based (e.g. lead rubber bearings, low and high damping rubber bearings) and sliding-based (e.g. flat sliders with restoring force capability (Eradiquake) and curved surface sliders).

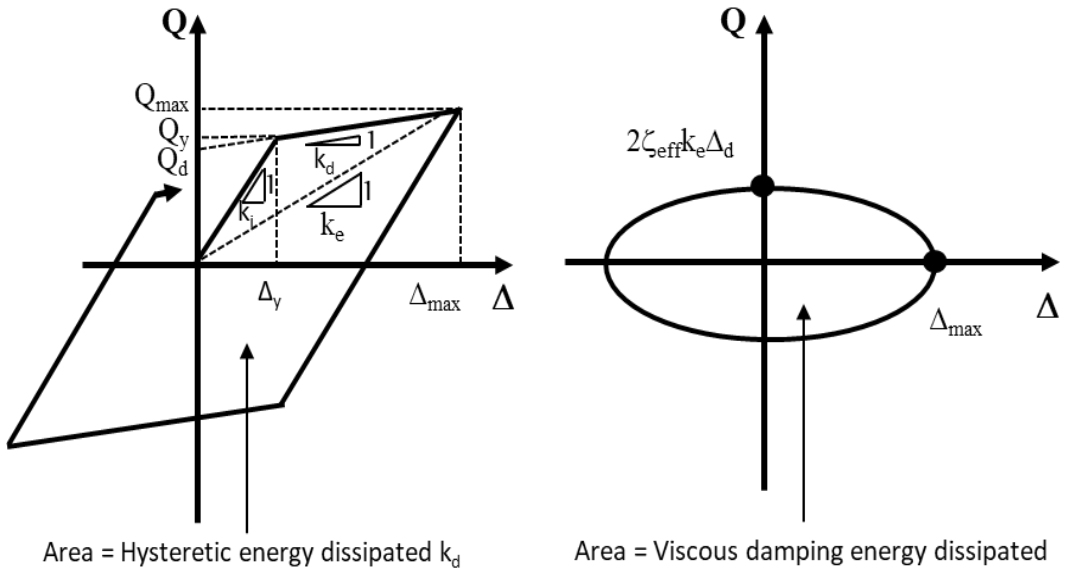

(a) *(b)*

Figure 1.1. (a) Idealized hysteresis loop of a typical isolator. (b) Hysteresis loop of a viscous damper

The force versus displacement hysteretic relationship of typical isolators similar to those listed above is generally idealized as bilinear in the analyses conducted for design as shown in Fig. 1.1 (a), where Q_d=characteristic strength, k_i=elastic stiffness, k_d=post-elastic stiffness, Q_y= yield force, Δ_y=yield displacement, Q_{max}=maximum (design) force and Δ_d= maximum (design) displacement of the isolator.

As stated earlier, iterative procedures based on linear elastic theories are frequently used for the analysis of seismic isolated structure. Such procedures require the equivalent linear properties of the seismic isolator, which is the effective stiffness, k_e, as shown in Fig. 1.1 (a). k_e, is defined as the slope of the dashed line connected from the origin to the point of maximum force on the hysteresis curve. Thus, k_e is obtained by dividing the maximum force, Q_{max}, by the maximum displacement, Δ_{max} of the isolator.

$$k_e = \frac{Q_{max}}{\Delta_{max}} = \frac{Q_y}{\Delta_{max}} + k_d \qquad \text{(Eq. 1.1)}$$

To take into consideration the hysteretic energy dissipated by the isolator at each cycle, an effective viscous damping ratio, ξ_e, is used in the iterative calculations based on linear elastic theory. The effective damping ratio, ξ_e, is obtained by setting up the area under the hysteresis curve of Fig. 1.1 (a) to the area under the hysteresis loop of a typical linear viscous damper in Fig. 1.1 (b).

$$\xi_e = \frac{4Q_y(\Delta_{max} - \Delta_y)}{2\pi k_e \Delta_{max}^2} \qquad \text{(Eq. 1.2)}$$

Equation 1.2 is derived based on the assumption that the excitation frequency is identical to the natural frequency of the equivalent linear system. (Jacobsen and Ayre, 1958). Accordingly, a response spectrum with a damping ratio equal to the effective damping ratio, ξ_e, is then used in the linear analyses to account for the hysteretic energy dissipated by the isolator. This is achieved by dividing the 5% damped design

spectrum by a damping reduction factor obtained for the calculated effective damping ratio

1.5. ELA Procedure for Seismic Isolated Structure

The ELA procedure, which is commonly followed for the design of seismic isolated structure, is outlined below for a single degree of freedom seismic isolated structure composed of an isolator supporting a rigid mass, m;

- Assume a maximum displacement, Δ_{max} for the isolator
- Substitute Δ_{max} and the properties of the isolator in equation 1.1 to calculate the effective stiffness, k_e of the isolator.
- Substitute Δ_{max}, k_e and the properties of the isolator in equation 1.2 to calculate the effective damping ratio, ξ_e.
- Calculate the effective period T_e of the seismic isolated structure as follows;

$$T_e = 2\pi\sqrt{\frac{m}{k_e}} \qquad \text{(Eq. 1.3)}$$

- Obtain a new Δ_{max} from the displacement response spectrum $S_D(\xi_e, T_e)$ defined as a function of effective damping ratio and effective period where, $S_D(\xi_e, T_e) = (4T_e^2/\pi^2)\, S_a(\xi_e = 0.05, T_e)/B$. In the above expression, $Sa(\xi_e = 0.05, T) = 5\%$ damped acceleration response spectrum, B= damping reduction factor.
- Compare the new Δ_{max} with the initially assumed one. If the difference between the two displacements is smaller than a predetermined tolerance level, then halt the iteration. Otherwise continue with the next round of iterations using the new maximum displacement.

1.6. Literature Review

Many research studies have been conducted to study the accuracy of the ELA results for seismic isolated structures subjected to far fault (Hwang and Sheng 1993; Hwang 1996; Hwang et al. 1997; Franchin et al. 2001) and NGM with FRDE (Hatzigeorgiou, G.D., 2010; Priestley, et al. 2007; Newmark, N.M., and Hall, W.J., 1982). As the

accuracy of ELA is generally controlled by the damping reduction factor, some of these studies focused on the effect of parameters such as the earthquake magnitude, distance to the governing fault, fault rupture mechanism, soil classifications of the site, duration of ground motion and number of cycles on the value of the damping reduction factor. As a result of such studies, new damping reduction equations have been proposed to improve the accuracy of ELA results. One of the first studies on damping reduction equations to improve the accuracy of ELA results have been performed by Newmark and Hall (1982) where an equation is proposed for ELA of structures subjected to NGM. Similarly, Lin and Chang (2003), Priestley et al. (2007), Cameron and Green (2007), Hatzigeorgiou (2010) and Hubbard and Mavroeidis (2011) have proposed damping reduction equations to improve the ELA results of structures. However, the proposed equations are either too simplistic (e.g. neglect many parameters including the properties of the seismic isolation system) or complicated (hard to apply in practice) and fail to produce accurate results over a broad range of isolator and ground motion parameters. Accordingly, in this study, a new damping reduction equation is proposed for the ELA of seismic isolated structures subjected to NGM with forward rupture directivity. Moreover the damping reduction equations or factors available in the literature and international design codes will be examined in detail in Chapter-3.

CHAPTER 2

PARAMETERS AND GROUND MOTIONS CONSIDERED IN THIS RESEARCH STUDY

2.1. Parameters Included in the Analyses

It is anticipated that the damping reduction equation for the ELA of seismic isolated structures subjected to NGM with FRDE, may be affected by many parameters such as; (i) the mass of the superstructure, m, (ii) the properties of the isolation system such as the characteristic strength, Q_d and the post elastic period, T_d, which is a function of the post elastic stiffness of the isolation system, k_d, and (iii) the properties of the NGM that is, the peak ground acceleration, A_p and pulse period T_p. which may be expressed as a function of the corner period, T_c of the design response spectrum. However, these parameters may be combined in a dimensionless form to simplify the damping reduction equation that will be developed as part of this research study.

Dimensionless analysis is a practical analytical method that may be used to represent many parameters in a simple form using only a few dimensionless variables. Makris and Black (2004a, b) used dimensional analysis method to completely describe the performance of a structural system with bilinear force-displacement relationship subjected to a pulse type excitation via four dimensionless terms. The proposed dimensionless terms are $R_1=\Delta_{max}/A_pT^2_p$, $R_2=mA_p/Q_d$, $R_3=\Delta_y/A_pT^2_p$, $R_4=T_p/T_s$, where T_s is the period of the structure based on its post elastic stiffness and all the other variables are described earlier. Within the context of this research study, R_2 and R_4, are used as dimensionless parameters in the development of the damping reduction equation. However, in these dimensionless parameters, the term T_p is replaced by the corner period, T_c, of the design response spectrum and the term T_s is replaced by the post elastic period, T_d, of the seismic isolated structures based on the post elastic

stiffness of the isolation system. The dimensionless term, R_2 describes the ratio of the seismic inertial forces acting on a rigid mass to the characteristic strength of the isolation system. In this research study, the weight of the superstructure is assumed as a constant equal to 10000 kN. However, the characteristic strength Q_d and the post elastic period T_d are varied between 200 kN – 1500 kN (5 different values: 200, 500, 700, 1000, 1500 kN) and 2 s. – 6 s (5 different values: 2,3,4,5,6 s.) respectively and the peak ground acceleration, A_p is varied between 0.2g and 1.5g (5 different values: 0.2, 0.5, 0.7, 1.0, 1.5 g). Therefore, 5×5×5=125 different cases are considered in this study. In addition, the soil type is also considered as a parameter in the selection of the ground motions, which makes the number of cases equal to, 125×3=375. Further details are presented in the following section.

2.2. Ground Motions Used in the Analyses and Their Smoothed Spectra

The NGM considered in this research study are sorted into three sets of ground motions according to their site soil classifications, namely, A&B, C and D. Due to the lack of ground motion data for site soil classifications A and B, these site soil classifications are combined into one set of seven NGM and each one of the other two site soil classifications are represented by a set of 11 NGM. Soil types E and F are not considered in this research study since such soft soil types are not suitable for seismic isolated structures due to the amplification of the response in the long period region. In the selection of the NGM, the distance to the fault is considered to be less than 20 km. Furthermore, the fault normal component is considered in the selection process to include FRDE. Moreover, the fault mechanism is not considered in the classification of the NGM due to lack of available NGM with FRDE data.

For each set of NGM, all the ground motions are first scaled to the same peak ground acceleration and then their average response spectrum is obtained. Then a smoothed spectrum is matched to the average response spectrum for each set of ground motions. This smoothed response spectrum is used in the ELA of seismic isolated structures performed as part of this research study. The smoothed response spectrum is

composed of three regions; (i) ascending or acceleration sensitive region, (ii) flat or velocity sensitive region and (iii) descending or displacement sensitive region. To obtain the smoothed response spectrum, first, a minimum least square power function is fitted to the average response spectrum within the displacement sensitive region of the response spectrum. Then, the spectral amplitude of the flat or velocity sensitive region of the smoothed spectrum is defined as the weighted average of the spectral accelerations of the average response spectrum within that region. The ascending or acceleration sensitive region of the smoothed response spectrum is formulated by fitting a minimum least square linear function to the average response spectrum within that region. The intersection points of the functions defining the smoothed response spectrum in these three regions identifies the first and second corner periods of the smoothed response spectrum. The acceleration response spectrum of each ground motion are shown in Fig. 2.2 (a), Fig. 2.3 (a) and Fig. 2.4 (a) for soil classifications A&B, C and D respectively and their average spectrum and the smoothed response spectrum for each set of ground motions are shown in Fig. 2.2 (b), Fig. 2.3 (b) and Fig. 2.4 (b) for soil classifications A&B, C and D respectively. These smoothed response spectra are used in the ELA of single degree of freedom seismic isolated structures for each site soil classification as part of the procedure to determine appropriate damping reduction factors that will be used in the development of damping reduction equation.

For the verification of the proposed damping reduction equation, nine additional NGM are selected and grouped into three ground motions according to their site soil classifications, namely, A&B, C and D. The properties of the ground motions used for the purpose of verification of the developed damping reduction equation are listed in Table 2.2. The smoothed response spectra of each sets of ground motions are then obtained as described above. This smoothed response spectrum is used in the ELA of seismic isolated structures performed as part of this research study. The acceleration response spectrum of each ground motion are shown in Fig. 2.5 (a), Fig. 2.6 (a) and Fig. 2.7 (a) for soil classifications A&B, C and D respectively and their average

spectrum and the smoothed response spectrum for each set of ground motions used for verification are shown in Fig. 2.5 (b), Fig. 2.6 (b) and Fig. 2.7 (b) for soil classifications A&B, C and D respectively.

Moreover, it’s noteworthy that these response spectra are different than those proposed in international design codes, especially with in the long period regions of the spectra for soft soil conditions. This is due to the fact that large event ground motions recorded on soft soils include increase seismic energy at long periods (Mestav et al. 2016).

Table 2.1. *NGM considered in the development of the damping reduction equation*

Soil Type	Earthquake	Station	Mw	R (km)	A_p (g)	T_p (s)	Avg. T_p (s)
A & B	San Fernando	Pacoima Dam (upper left abut)	6.6	1.8	1.43	1.6	2.01
	Loma Prieta	Gilroy - Gavilan Coll.	6.9	10.0	0.29	1.8	
	Loma Prieta	Gilroy Array #1	6.9	9.6	0.43	1.2	
	Cape Mendocino	Petrolia	7.0	8.2	0.61	3.0	
	Landers	Lucerne	7.3	2.2	0.71	5.1	
	Northridge-01	Pacoima Dam (downstr)	6.7	7.0	0.50	0.5	
	Northridge-01	Pacoima Dam (upper left)	6.7	7.0	1.38	0.9	
C	Coyote Lake	Gilroy Array #6	5.7	3.1	0.45	1.2	2.47
	Chi-Chi- Taiwan	CHY006	7.6	9.8	0.31	2.6	
	Morgan Hill	Gilroy Array #6	6.2	9.9	0.24	1.2	
	Morgan Hill	Coyote Lake Dam (SW Abut)	6.2	0.5	0.81	1.0	
	Loma Prieta	LGPC	6.9	3.9	2.94	3.0	
	Loma Prieta	Saratoga - Aloha Ave	6.9	8.5	0.36	4.5	
	Loma Prieta	Saratoga - W Valley Coll.	6.9	9.3	0.4	1.9	
	Northridge-01	Jensen Filter Plant Generator	6.7	5.4	0.52	3.5	
	Northridge-01	LA Dam	6.7	5.9	0.58	1.7	
	Northridge-01	Sylmar - Converter Sta East	6.7	5.2	0.84	3.5	
	Northridge-01	Sylmar - Olive View Med FF	6.7	5.3	0.73	3.1	

Soil Type	Earthquake	Station	Mw	R (km)	A_p (g)	T_p (s)	Avg. T_p (s)
D	Imperial Valley	Aeropuerto Mexicali	6.5	0.3	0.36	2.4	2.81
	Imperial Valley	Agrarias	6.5	0.7	0.31	2.3	
	Imperial Valley	El Centro Array #8	6.5	3.9	0.47	5.4	
	Imperial Valley	El Centro Differential Array	6.5	5.1	0.42	5.9	
	Superstition Hills-02	El Centro Imp. Co. Cent	6.5	18.2	0.31	2.4	
	Superstition Hills-02	Parachute Test Site	6.5	0.9	0.42	2.3	
	Erzincan- Turkey	Erzincan	6.7	4.4	0.49	2.7	
	Loma Prieta	Gilroy Array #2	6.9	11.1	0.41	1.7	
	Northridge-01	Newhall - Fire Sta.	6.7	5.9	0.72	2.2	
	Northridge-01	Newhall - W Pico Canyon Rd.	6.7	5.5	0.43	2.4	
	Northridge-01	Rinaldi Receiving Sta.	6.7	6.5	0.87	1.2	

Table 2.2. *NGM considered in the verification of the damping reduction equation*

Soil Type	Earthquake	Station	Mw	R (km)	A_p (g)	T_p (s)	Avg. T_p (s)
A & B	Kocaeli Turkey	Izmit	7.5	7.2	0.23	5.4	3.00
	Loma Prieta	Los Gatos - Lexington Dam.	6.9	5.0	0.44	1.6	
	L'Aquila Italy	L'Aquila – Parking	6.3	5.4	0.34	2.0	

Soil Type	Earthquake	Station	Mw	R (km)	A_p (g)	T_p (s)	Avg. T_p (s)
C	Irpinia Italy-01	Bagnoli Irpinio	6.9	8.1	0.13	1.7	2.03
	Chi Chi Taiwan	CHY074	6.2	6.0	0.32	2.4	
	Bam Iran	Bam	6.6	1.7	0.81	2.0	
D	Northridge-01	Newhall - W Pico Canyon Rd.	6.7	5.5	0.42	3.0	3.00
	Kobe Japan	Port Island	6.9	3.3	0.35	2.8	
	Denali Alaska	TAPS Pump Station #10"	7.9	2.7	0.33	3.2	

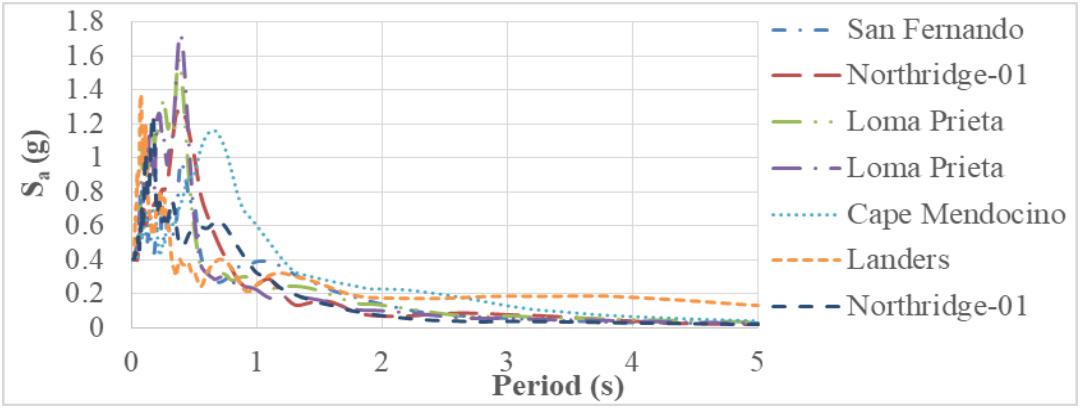

(a)

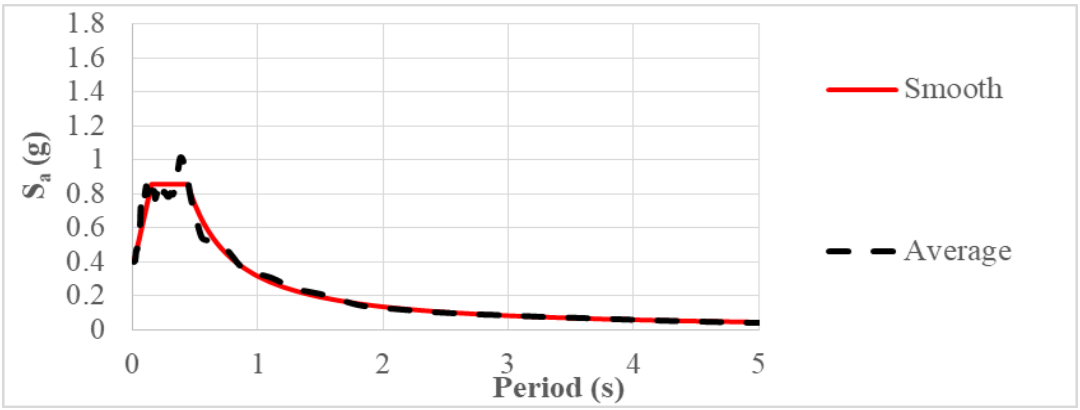

(b)

Figure 2.1. Ground motions considered in the development of the damping reduction equation for soil types A&B (a) Response spectra (b) average and smoothed spectra

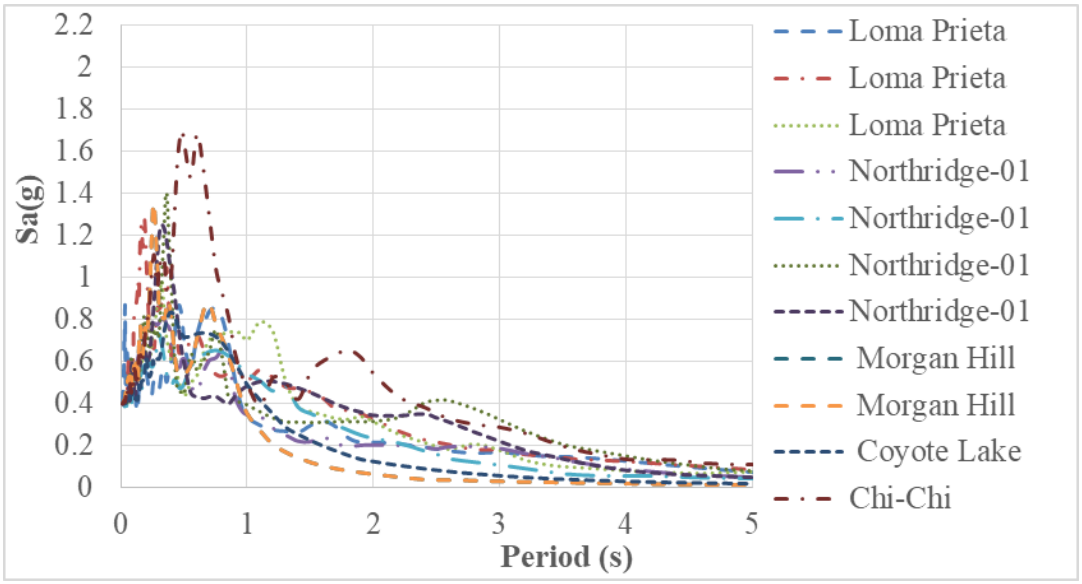

(a)

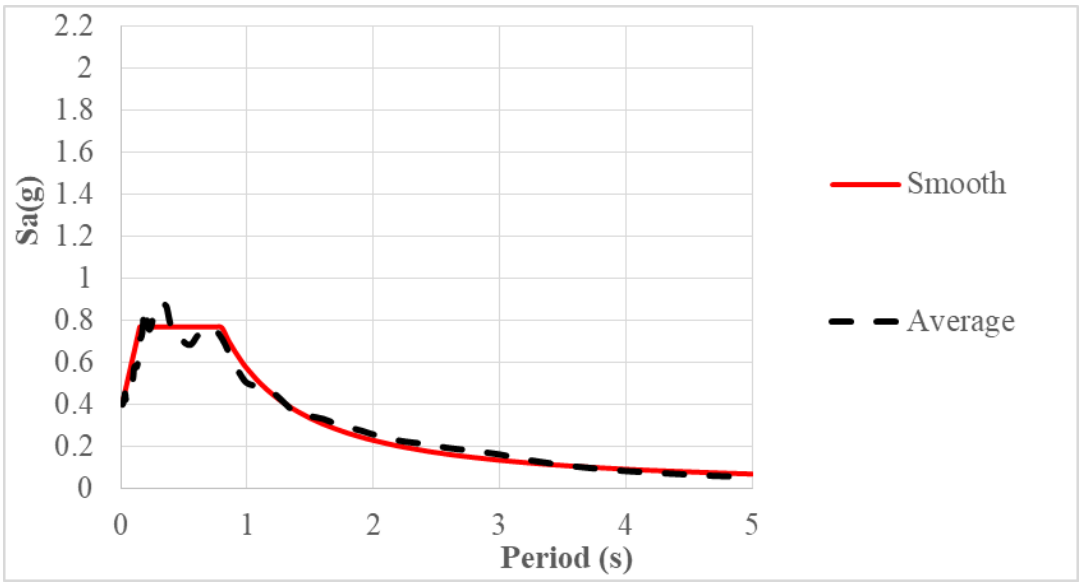

(b)

Figure 2.2. Ground motions considered in the development of the damping reduction equation for soil type C (a) Response spectra (b) average and smoothed spectra

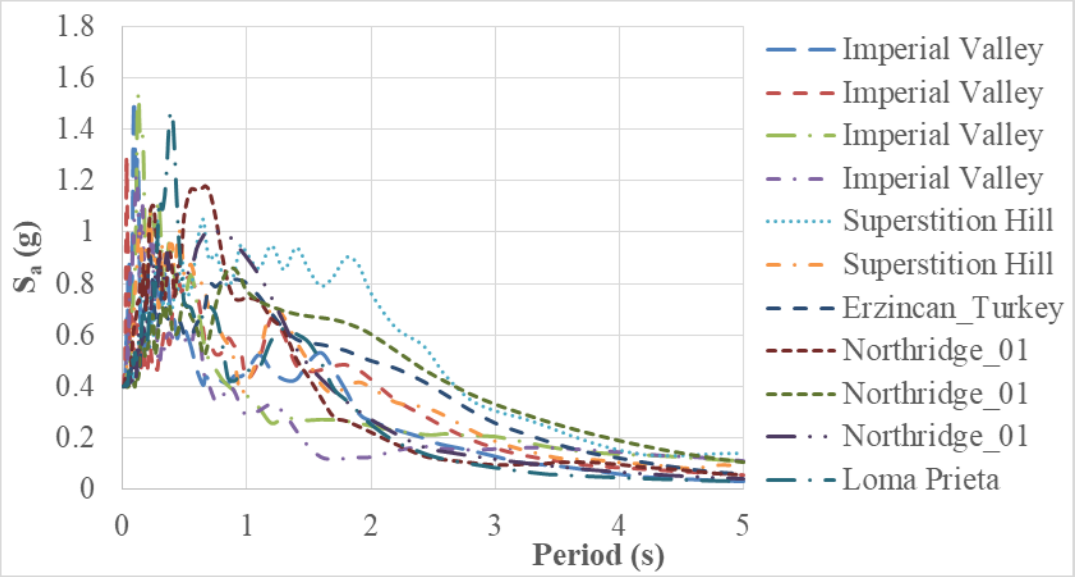

(a)

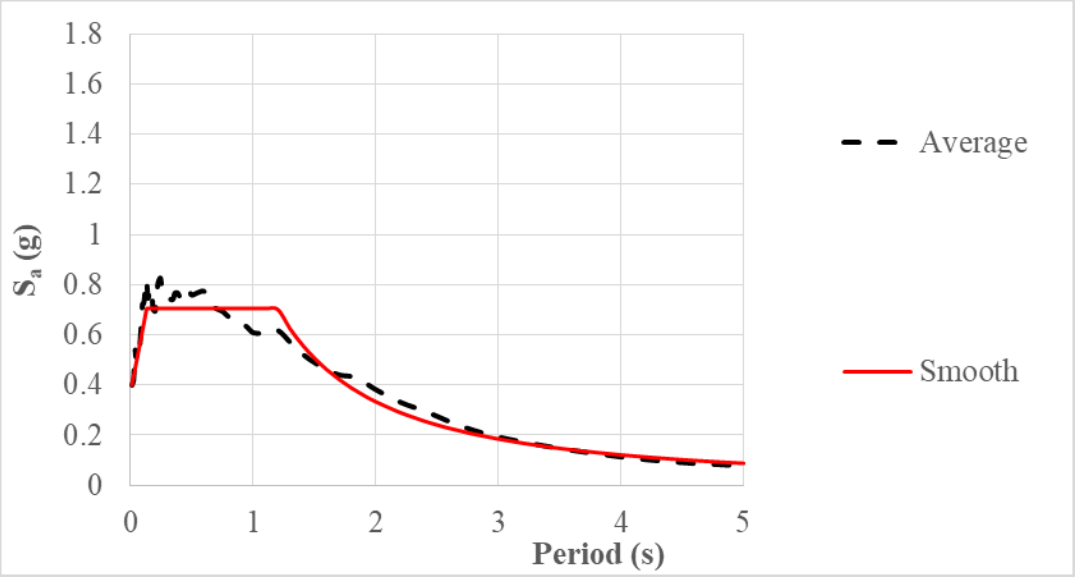

(b)

Figure 2.3. Ground motions considered in the development of the damping reduction equation for soil type D (a) Response spectra (b) average and smoothed spectra

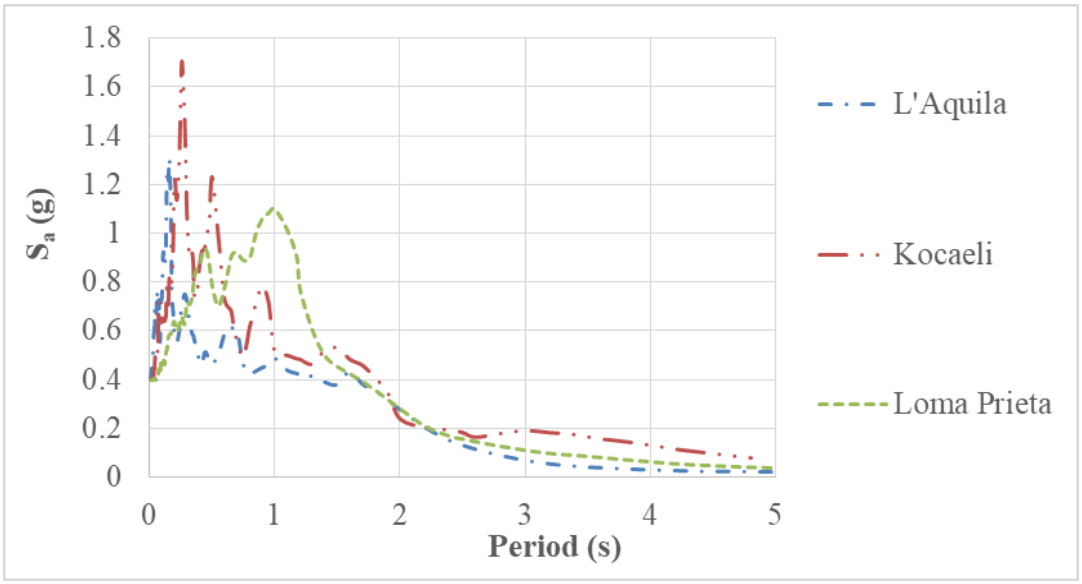

(a)

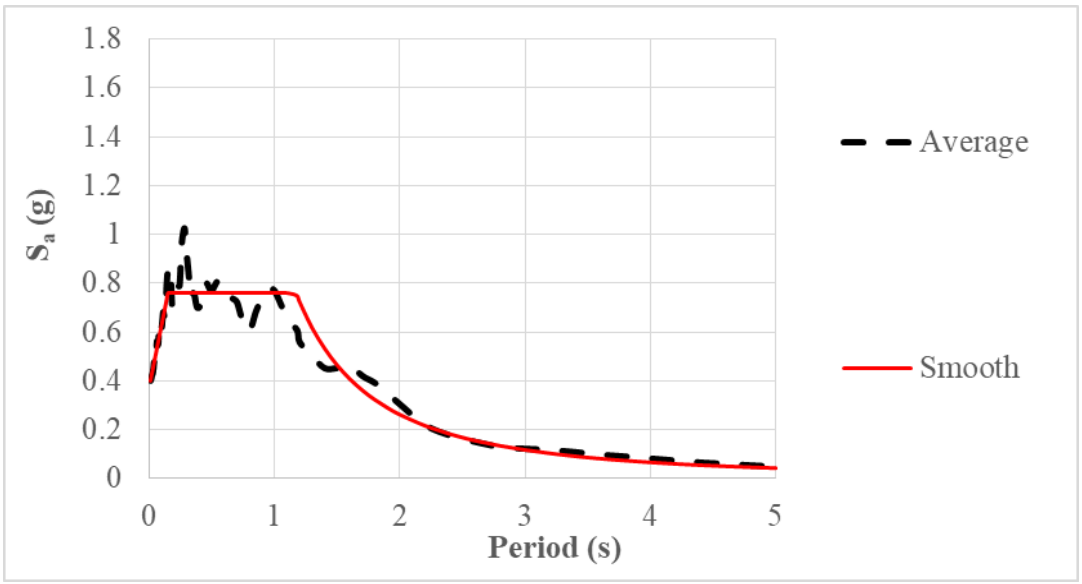

(b)

Figure 2.4. Ground motions considered in the verification of the damping reduction equation for soil types A&B (a) Response spectra (b) average and smoothed spectra

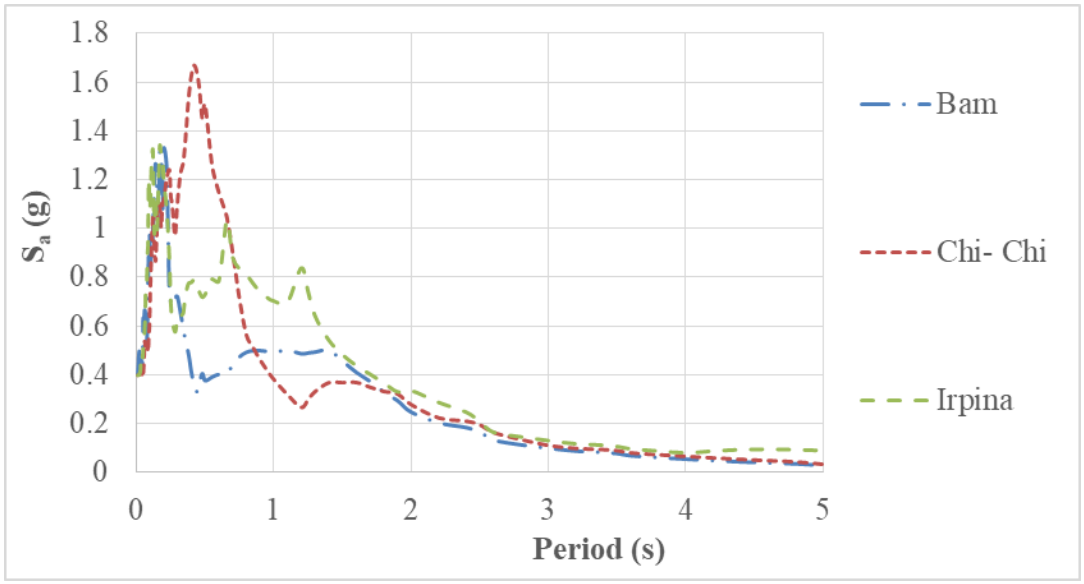

(a)

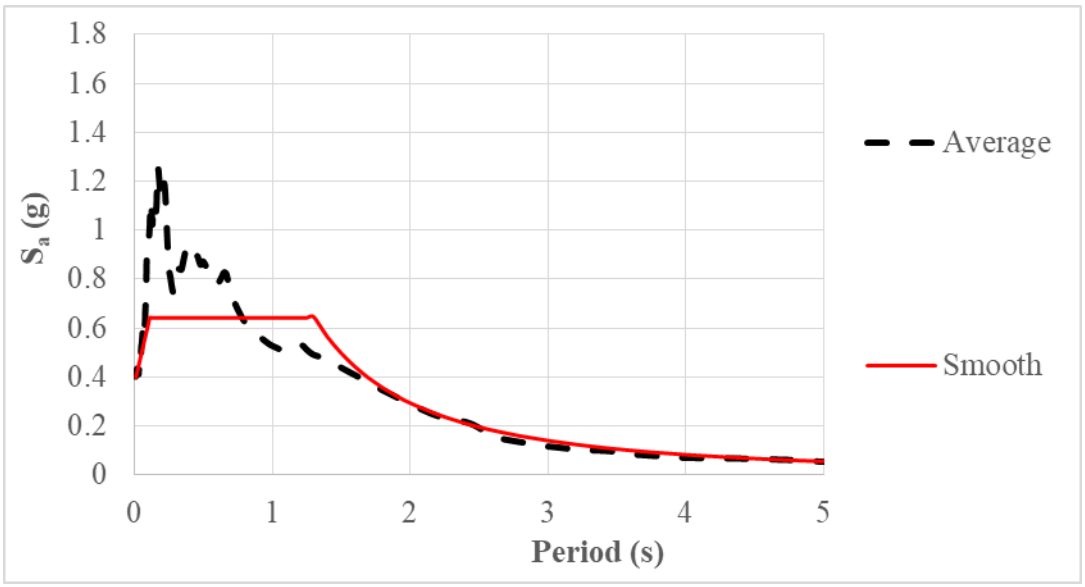

(b)

Figure 2.5. Ground motions considered in the verification of the damping reduction equation for soil type C (a) Response spectra (b) average and smoothed spectra

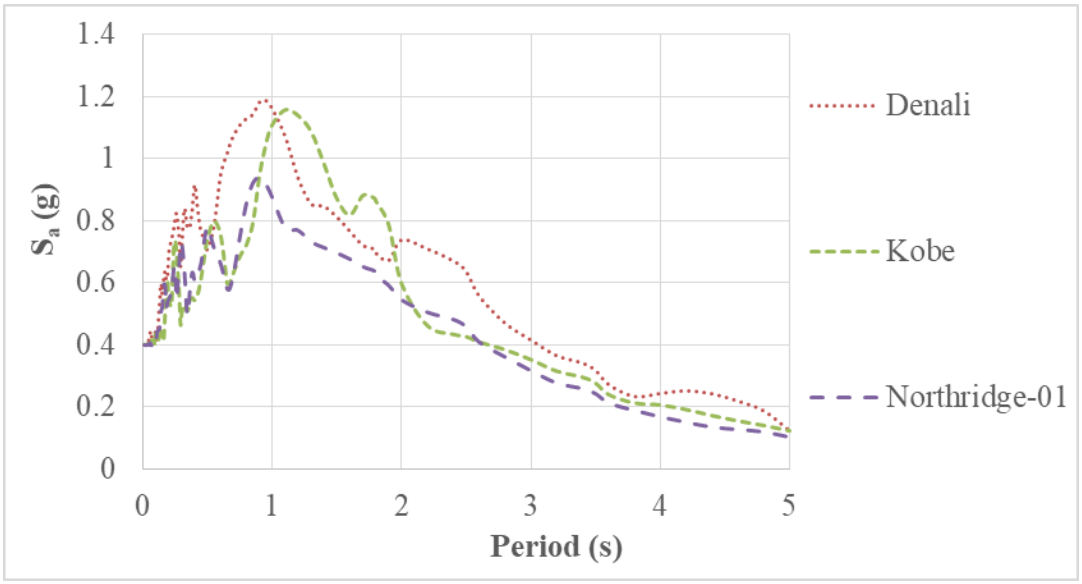

(a)

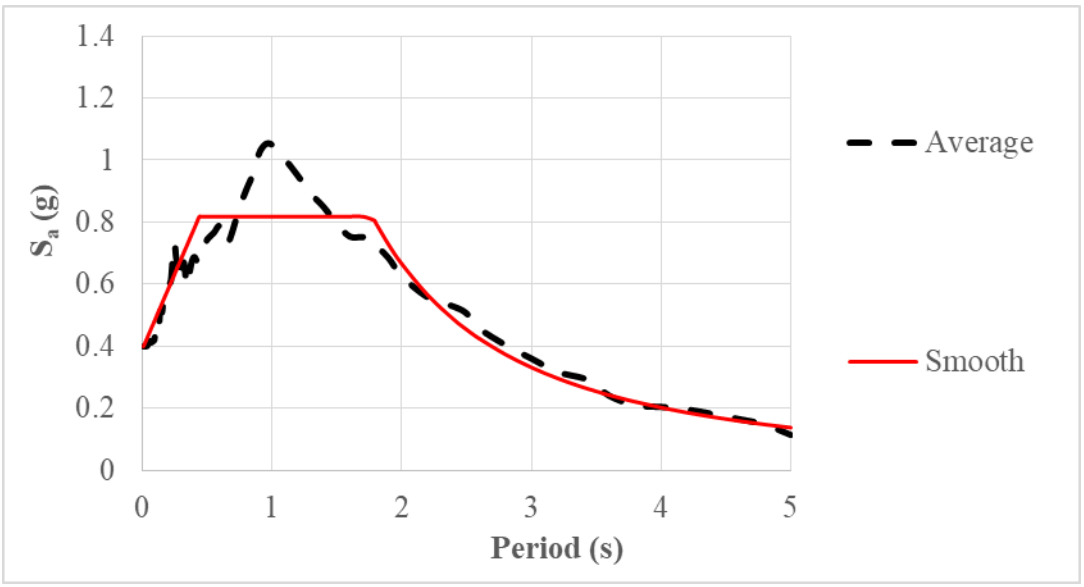

(b)

Figure 2.6. Ground motions considered in the verification of the damping reduction equation for soil type D (a) Response spectra (b) average and smoothed spectra

CHAPTER 3

DAMPING REDUCTION FACTORS AND EQUATIONS IN THE LITERATURE AND DESIGN CODES

3.1. Available Damping Reduction Factors and Equations in the Literature and Design Codes

In this section, damping reduction factors or equations available in various design standards as well as those proposed by various researchers are discussed. While AASHTO (2014) and EN 15129 (2010) use equations to define the damping reduction factor as a function the effective damping ratio, ASCE 7-16 (2016) and NEHRP (2009) present the damping reduction factor in a table form for various effective damping ratios ranging between 2% to 50%. The equations used in AASHTO (2014) and EN 15129 (2010) are presented in Equations 3.1 and 3.2, respectively.

$$B = \left(\frac{\xi_e}{0.05}\right)^{0.3} \quad \text{(Eq. 3.1)}$$

$$B = \sqrt{\frac{2+\xi_e}{7}} \quad \text{(Eq. 3.2)}$$

The effective damping ratio versus damping reduction factors presented in ASCE 7-16 (2016) and NEHRP (2009) are tabulated in Table 3.1. In the same table, the damping reduction factors used in all the aforementioned design specifications are also compared. It is observed that the damping reduction factors calculated for various effective damping ratios are similar except for EN15129 (2010) where the damping reduction factors for effective damping ratios ranging between 5% and 30% are approximately 10% larger than those of the others. However, none of these damping reduction factors or equations are specifically designed to take into consideration the

effect of intense, long duration velocity pulses present in NGM with FRDE on the isolator displacements.

Table 3.1. Damping reduction factors for various design standards

Effective Damping Ratio ξe	**Damping Reduction Factor**			
	ASCE 7-16 (2016)	**NEHRP (2009)**	**AASHTO (2014)**	**EN 15129 (2010)**
2	0.80	-	0.76	0.76
5	1.00	1.00	1.00	1.00
10	1.20	1.20	1.23	1.31
20	1.50	1.50	1.52	1.77
30	1.70	1.70	1.71	2.14
40	1.90	1.90	1.87	-
50	2.00	2.00	2.00	-

Several researchers have developed damping reduction equations or factors for the ELA of structures subjected to NGM with FRDE. Details of these proposed equations are given as follows;

Newmark and Hall (1982) suggested a damping reduction equation for 20% or less viscous damping ratio for the constant acceleration region, constant velocity region and constant displacement region of the design spectrum as follows;

$B = 1/(1.514 - 0.321 \ln(\xi_e))$ (For constant acceleration region) (Eq. 3.3.a)

$B = 1/(1.400 - 0.248 \ln(\xi_e))$ (For constant velocity region) (Eq. 3.3.b)

$B = 1/(1.309 - 0.194 \ln(\xi_e))$ (For constant displacement region) (Eq. 3.3.c)

Although the set of equations proposed by Newmark and Hall (1982) are simple, they are only valid for 20% or less viscous damping ratios and composed of three distinct expressions for various regions of the design response spectrum.

Lin and Chang (2003) proposed a damping reduction equation, which is a function of the effective period and damping ratio valid for the range of 2% and 50% damping as presented below;

$$B = \frac{(T+1)^{0.65}}{(T+1)^{0.65} - (1.303 + 0.436 \ln(\xi_e))T^{0.30}} \quad \text{(Eq. 3.4)}$$

More than 1000 ground acceleration time histories with a source to site distance ranging between 0.1 km and 100 km. was used in the development of the equation. Therefore, the equation proposed by Lin and Chang (2003) was developed using both near and far fault ground motions. Thus, it may not be suitable solely for the ELA of structures subjected to NGM with FRDE.

Priestley et al. (2007) proposed a damping reduction factor equation, which is a function of the effective damping ratio as follows;

$$B = \left(\frac{2+\xi_e}{7}\right)^{0.25} \quad \text{(Eq. 3.5)}$$

The equation is simple to use as it is only a function of the effective damping ratio. However, it lacks parameters related to structure, design spectrum and isolator properties.

Cameron and Green (2007) proposed a table for the damping reduction factor, which varies with the site soil classification, earthquake magnitude and equivalent viscous damping ratio. For the evaluation of this table, 1268 ground motions from 47 earthquake records were used. The viscous damping range of this table is in between 2% and 50%. However, since the proposed damping reduction factor is tabulated as a function of the magnitude of the ground motion, the use of such an approach is limited in practice.

Hatzigeorgiou (2010) proposed a set of damping reduction equations, which are functions of the effective period and damping ratio. Three sets of ground motions,

namely far fault, artificial records and near fault records, were used in the development of each damping reduction equation. The one developed using NGM is given below:

$$B = \frac{1}{1+(\xi_e-5)[1-0.36227ln(\xi_e)+0.03495]\left[-0.04517+0.3454ln(T)-0.00240\left(ln(T)\right)^2\right]} \quad \text{(Eq. 3.6)}$$

The main disadvantages of this equation is that it lacks the isolator and design spectrum parameters and it is quite complicated.

Hubbard and Mavroeidis (2011) proposed two damping reduction equations for two ranges of effective damping ratios, which are functions of the effective period, velocity pulse period of the ground motion and damping ratio as follows;

$$B = 3.4\,\frac{\xi_e{}^{1.3}}{(\frac{T}{T_p})^{1.3}} + 1 \quad \text{(For } 0.10 \le \xi_e \le 0.50\text{)} \quad \text{(Eq. 3.7.a)}$$

$$B = 2\,\frac{\left(\xi_e+0.3\right)^{1.5}}{(\frac{T}{T_p})^{1.3}} + 1 \quad \text{(For } 0.50 \le \xi_e \le 1.00\text{)} \quad \text{(Eq. 3.7.b)}$$

The equations proposed by Hubbard and Mavroeidis (2011) are simple to use but they lack the isolation system properties and involve the velocity pulse period of the ground motion, which is not available for the ELA of seismic isolated structures using a design spectrum.

The damping reduction equations proposed by Newmark & Hall (1982), Priestley et al. (2007), Hatzigeorgiou (2010) and Hubbard and Mavroeidis (2011) as well as the equation proposed in this study are used in ELA of various seismic isolated structures and the results are compared with those obtained from NLTHA of the same structures to demonstrate the comparative accuracy of the proposed equation in predicting the actual responses from NLTHA. The damping reduction equations proposed by Lin and Chang (2003) and Cameron and Green (2007) were not employed in the comparative assessment of the proposed damping reduction equation as the first one was developed using a mixture of far and NGM and the latter one employs the

magnitude of the earthquake as a parameter, which is not available for the ELA of seismic isolated structures using a design spectrum

3.2. Assessment of the Available Damping Reduction Equations in the Literature and Design Codes

In this section, the accuracy of the damping reduction equations available in the literature and design codes are assessed. These damping reduction equations are those proposed by Hatzigeorgiou (2010) Newmark & Hall (1982), Priestley et al. (2007), Hubbard& Mavroeidis (2011), AASHTO (2014) and EN 15129 (2010). The displacements obtained from the ELA of single degree of freedom seismic isolated structures using the damping reduction equations available in the literature and design codes are compared with those obtained from NLTHA. The analyses are performed for all the range of parameters (mA_p/Q_d and T_d) and ground motions considered in this research study. The NLTHA of the seismic isolated structures are conducted using the program SAP2000 (2015). A total of 3625 NLTHA and 2250 ELA are conducted for six damping reduction equations. The comparative analyses results are presented in a bar chart form as the ratio of the ELA results to the average of the results from NLTHA for each site soil classification A&B, C and D in Fig. 3.1 (a), (b) and (c) respectively and for the average of the results from all the analyses regardless of the site soil classification in Fig. 3.1 (d). It is noteworthy that each bar in Fig 3.1 contains the average of the ELA / NLTHA ratios for all the range of mA_p/Q_d and T_d parameters considered in this study.

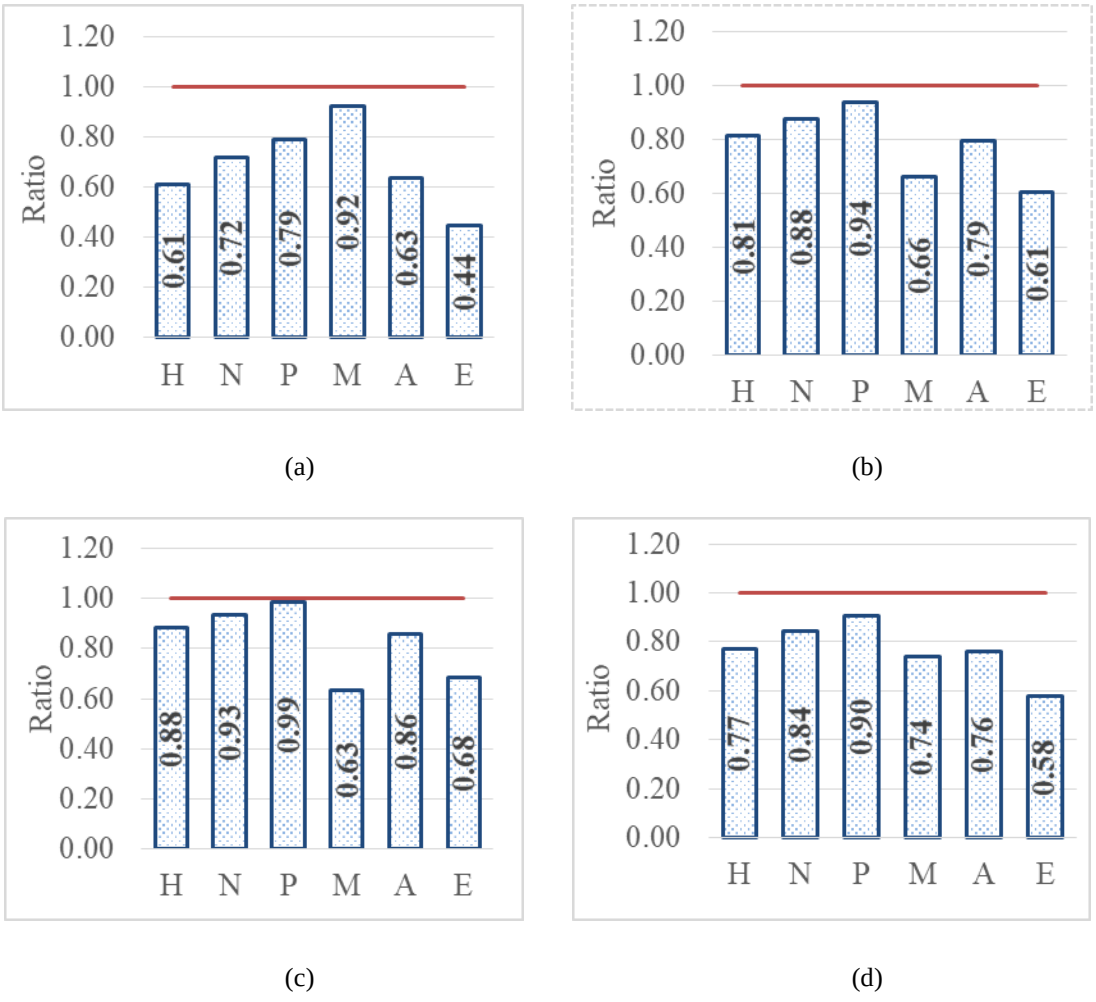

Figure 3.1. Ratio of displacement results of ELA with available damping reduction equations to displacement results NLTHA for site soil classifications (a) A&B, (b) C, (c) D, (d) Average from all site soil classifications. (H= Hatzigeorgiou (2010), N= Newmark & Hall (1982), P=Priestley et al. (2007), M=Hubbard & Mavroeidis (2011), A=AASHTO (2014), E= EN 15129 (2010))

Fig. 3.1 reveals that ELA performed using the damping reduction equations presented in AASHTO (2014) and EN 1529 (2010) severely underestimates the isolator displacements. This is expected since these equations have been developed without the consideration of directivity effect and associated intense velocity pulses specific to NGM. The difference between the ELA and NLTHA results is as much as 37% in the case of AASHTO (2014) and 66% in the case of EN 15129 (2010) for stiff site soil conditions. For softer site soil conditions, the discrepancy between the ELA and NLTHA results are less exaggerated but still significant.

In the case of four damping reduction equations employed in this study, the one proposed by Priestley et al. (2007) yields the most accurate displacement responses compared to those from NLTHA. However, ELA performed using the equation proposed by Priestley et al. (2007) underestimates the displacement response by 21% for soil classifications A&B (stiff soil conditions), by 6% for soil classification C and 1% for soil classification D (soft soil conditions) and on the average by 10% for all the soil classifications. Thus, while the equation proposed by Priestley et al. (2007) produces reasonably good estimates of the displacement response for soft soil conditions, it underestimates the displacement response noticeably for stiff soil conditions. On the contrary, ELA conducted using the damping reduction equation proposed by Hubbard and Mavroeidis (2011) produces reasonably good estimates of the displacement response for stiff soil conditions (underestimates by only 8%), but underestimates the displacement response remarkably for soft soil conditions (underestimates by 37%). Similar to the damping reduction equation proposed by Priestley et al. (2007), those proposed by Hatzigeorgiou (2010) and Newmark and Hall (1982) also produce better estimates of the displacement responses for soft soil conditions than those for stiff soil conditions, but with lesser accuracy compared to the displacement responses obtained by using the equation proposed by Priestley et al. (2007) .

Based on the above discussion, it may be concluded that neither the damping reduction equations available in the literature nor the ones given in AASHTO (2014) and EN15129 (2010) produce accurate estimates of the actual displacement responses of seismic isolated structures subjected to NGM with FRDE. Therefore, a damping reduction equation that is capable of producing reasonably good estimates of displacement responses regardless of the site soil classification is urgently needed.

CHAPTER 4

DEVELOPMENT OF THE PROPOSED DAMPING REDUCTION EQUATION

4.1. General

In this section, a damping reduction equation for the ELA of seismic isolated structures subjected to NGM with FRDE is developed. For this purpose, first a single degree of freedom system with an infinitely rigid mass (weight = 10000 kN) on an isolator is assumed to represent seismic isolated structures. This simple system is used to decouple the response of the seismic isolated structures from other parameters such as superstructure properties in the case of buildings and substructure properties in the case of bridges. This enabled to build a direct relationship between the damping reduction factor, B and the nonlinear response of the seismic isolated structures. Next, NLTHA of single degree of freedom systems with various properties as determined by the dimensionless parameters mA_p/Q_d and T_p/T_d are performed using the 29 ground motions considered in this study to estimate the nonlinear displacements of the single degree of freedom systems. This resulted in 3625 displacement data points. However, the average of the maximum displacements from each set of ground motions is used to calculate the nonlinear displacement responses of the single degree of freedom systems for each site soil classification. Thus, the number of displacement data points used in the development of the damping reduction equation is 875 / 7 + 1375 / 11 + 1375 / 11 = 375. Then, the average of the maximum displacements obtained from the NLTHA using each set of ground motions is assumed to be equal to the displacement of an equivalent linear system. Accordingly, the procedure outlined below is used to calculate the damping reduction factor such that when this factor is used in an ELA procedure, a displacement equal to that from NLTHA would be obtained;

(i) Using the displacement, Δ_{NLTHA}, obtained from NLTHA calculate the effective stiffness, k_e, of the single degree of freedom seismic isolated structures under consideration as follows. $k_e=Q_d/\Delta_{NLTHA} + k_d$

(ii) Calculate the effective period $T_e=2\pi(m/k_e)^{0.5}$

(iii) Obtain the spectral acceleration S_a corresponding to the calculated effective period from the smoothed response spectrum.

(iv) Convert the spectral acceleration to spectral displacement as: $S_d=(T_e^2/4\pi^2)\, S_a$. Note that the calculated spectral displacement is for 5% damping. To obtain the spectral displacement for the effective damping produced by the energy dissipation of the seismic isolation system, S_d should be divided by the damping reduction factor, B.

(v) Knowing that $S_d/B=\Delta_{NLTHA}$, the damping reduction factor is calculated as $B=S_d/\Delta_{NLTHA}$

The above procedure is followed to obtain the damping reduction factors as a function of various parameters namely ξ_e, mA_p/Q_d. and T_p/T_d. The results are presented in the following section.

4.2. Variation of Damping Reduction Factors as a Function of Various Parameters

The variation of the damping reduction factor, *B*, as a function the effective damping ratio, ξ_e as well as the dimensionless parameters, mA_p/Q_d. and T_p/T_d is presented in Fig.4.1. The plots in Fig.4.1 are used to discover the form of the proposed damping reduction equation.

Fig. 4.1 (a) depicts the variation of the damping reduction factor as a function of the effective damping ratio. The figure shows that the damping reduction factor increases with increasing effective damping ratio. This is expected since large damping results in lower spectral amplitudes. Nonlinear minimum least square fit of the B-ξ_e data reveals that the relationship between B and ξ_e, is in the form of a power function,

$Y=aX^b$. This relationship is considered in the development of the damping reduction equation.

A similar plot, that relates the variation of B as a function of mA_p/Q_d is presented in Fig 4.1 (b). As observed from the figure, the damping reduction factor decreases as the dimensionless parameter mA_p/Q_d increases. This is expected since for larger Q_d values, the area under the hysteresis loop and associated damping increases. Thus, the damping reduction factor, B increases for smaller mA_p/Q_d values. Nonlinear minimum least square fit of the B- mA_p/Q_d data in Fig. 4.1 (b) reveals that the relationship between B and mA_p/Q_d is also in the form of a power function, $Y=aX^b$. Thus, such a relationship between B and mA_p/Q_d is considered in the development of the proposed damping reduction equation.

Fig. 4.1 (c) shows the variation of B as a function of T_p/T_d. The general trend of the plot indicates an increase in the value of B with increasing T_p/T_d ratio. For a single degree of freedom system with a post-elastic period, T_d, the T_p/T_d ratio increases as the pulse period, T_p of the NGM increases. For ground motions with large pulse periods, the time duration of the pulse type seismic forces above the threshold of the yield level of the seismic isolated structures increases as depicted in Fig. 4.1 (d). This phenomenon results in larger inelastic displacements and associated larger damping due to pulse effect. Consequently, the damping reduction factor, B increases for larger T_p/T_d ratios. Although the nonlinear minimum least square fit of the B- T_p/T_d data in Fig. 4.1 (c) looks more or less linear, a power function, in the form of $Y=aX^b$ is used to define the relationship between B and T_p/T_d ratio considering the ability of power functions to fit any form of variation. Such an approach is followed to simplify the form of the proposed damping reduction equation.

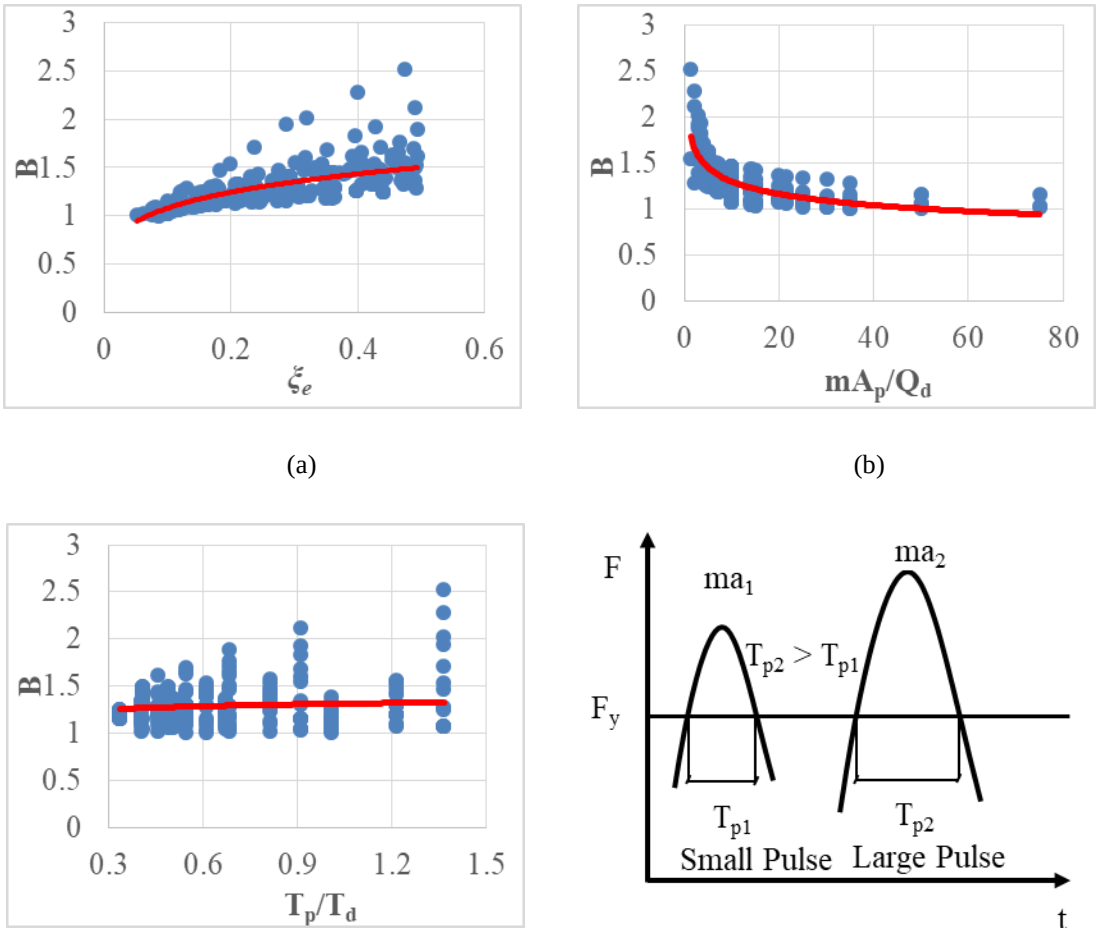

(a) (b)

(c) (d)

Figure 4.1. Variation of the damping reduction factor with (a) ξe, (b) mA_p/Q_d, (c) T_p/T_d, (d) Time duration of small and large pulses above the threshold of yielding

4.3. Development of the Proposed Damping Reduction Equation

In light of the observations in the preceding section and knowing that for an effective damping ratio of $\xi_e=0.05$, the damping reduction factor must assume the value of unity ($B=1.0$), the proposed damping reduction equation is assumed to have the following form.

$$B = 1 + a(\xi_e - 0.05)^{b1}\left(\frac{mA_p}{Q_d}\right)^{b2}\left(\frac{T_p}{T_d}\right)^{b3} \quad \text{(Eq. 4.1)}$$

Where a1, a2, a3, b1, b2 and b3 are constants to be determined via regression analyses using the available data. To obtain the constants in equation 4.1, first (*B-1*) values,

which are obtained from the ELA back-calculations, are plotted as a function of (ξ_e - 0.05) as shown in Fig. 4.2 (a). Then, the minimum least square fit of the logarithm of the (ξ_e - 0.05) – (*B*-1) data is performed to obtain the following equation;

$$F_1 = 1.0772(\xi_e - 0.05)^{0.8728} \quad \text{(Eq. 4.2)}$$

The above equation, which is plotted using a thick solid line in Fig. 4.2 (a), gives (*B*-1) as a function of (ξ_e - 0.05). The term (ξ_e - 0.05)$^{0.8728}$ in Equation 4.2 represents the term (ξ_e - 0.05)^{b1} in Equation 4.1. Thus b_2 = 0.8728. The scatter of data in Fig. 4.2 (a) with respect to the plot of Equation 4.2 is mainly due to the error introduced by the absence of the other parameters in the equation. This error will be corrected by involving the effect of the remaining parameters in the equation. For this purpose, first, the ratio F_2, of the (*B*-1) results to those obtained from Equation 4.2 is calculated as;

$$F_2 = \frac{B-1}{F_1} \quad \text{(Eq. 4.3)}$$

This is done to decouple the damping reduction factor results from the effect of the term (ξ_e - 0.05). Then the ratio F_2 is plotted as a function of the dimensionless parameter of mass, peak ground acceleration and characteristic strength of isolator (mA_p/Q_d) in Fig. 4.2 (b). Next, the minimum least square fit of the logarithm of the data presented in Fig. 4.2 (b) is performed to obtain the following equation;

$$F_2 = 1.7903\left(\frac{mA_p}{Q_d}\right)^{-0.246} \quad \text{(Eq. 4.4)}$$

The above equation is plotted using a thick solid line in Fig. 4.2 (b). The term (mA_p/Q_d)$^{-0.246}$ in Equation 4.4 represents the term (mA_p/Q_d) ^{b2} in Equation4.1. Thus, b2 = -0.246. Next, to obtain the term b_3, a new ratio, F_3 is calculated as;

$$F_3 = \frac{B-1}{F_1 \times F_2} \quad \text{(Eq. 4.5)}$$

Then, the ratio F_3, is plotted as a function of the pulse period of the NGM divided by the post elastic period of the isolator (T_p/T_d), in Fig. 4.2 (c). Next, the minimum least

square fit of the logarithm of the data presented in Fig. 4.2 (c) is performed to obtain the following equation;

$$F_3 = 1.1994\left(\frac{T_p}{T_d}\right)^{0.4033} \qquad \text{(Eq. 4.6)}$$

The above equation is plotted using a thick solid line in Fig. 4.2 (c). The term $(T_p/T_d)^{0.4033}$ in Equation 4.6 represents the term $(T_p/T_d)^{b3}$ in Equation 4.1. Thus, b_3=0.4033. The damping reduction factor of seismic isolated structures subjected to NGM with FRDE is obtained by solving for *B* in Equation 4.5 (B=1+ F1 × F2 × F3). Accordingly the constant, a in Equation 4.1 is obtained by multiplying the coefficients in front of the terms, (ξ_e-0.05), (mA_p/Q_d) and (T_p/T_d) in Equations 4.2, 4.4 and 4.6, respectively. Thus, a=1.0772×1.7903×1.1994=2.3131. After rounding off the calculated coefficients and simplifications, the final form of the damping reduction equation becomes as follows;

$$B = 1 + 2.3 \times (\xi_e - 0.05)^{0.85}\left(\frac{Q_d}{mA_p}\right)^{0.25}\left(\frac{T_p}{T_d}\right)^{0.40} \qquad \text{(Eq. 4.7)}$$

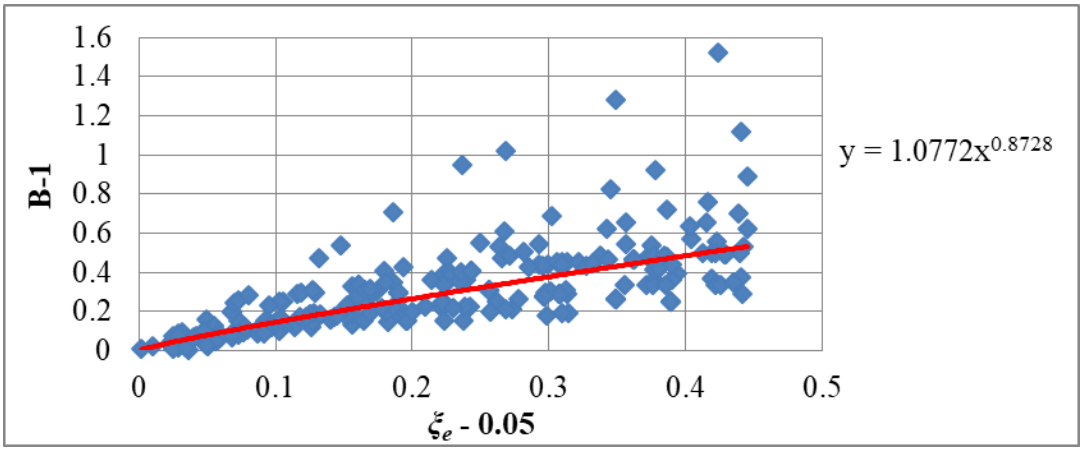

(a)

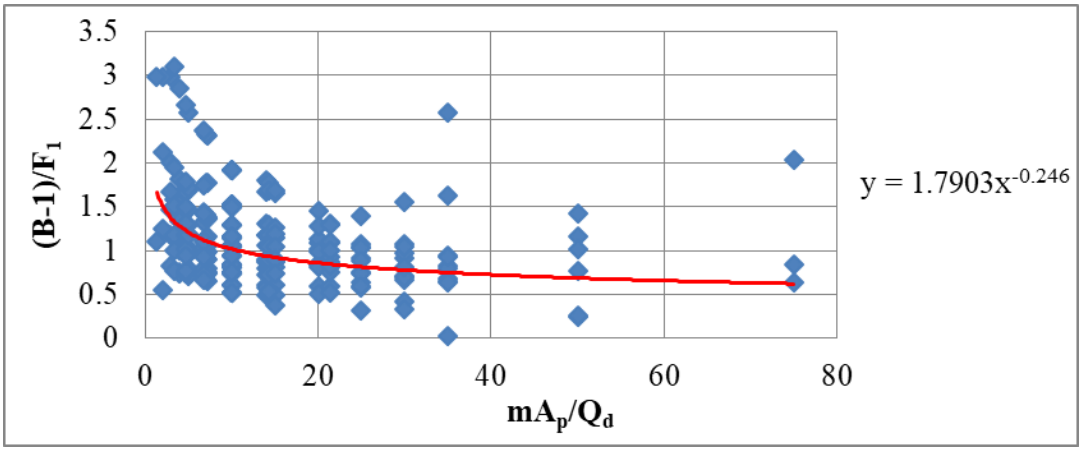

(b)

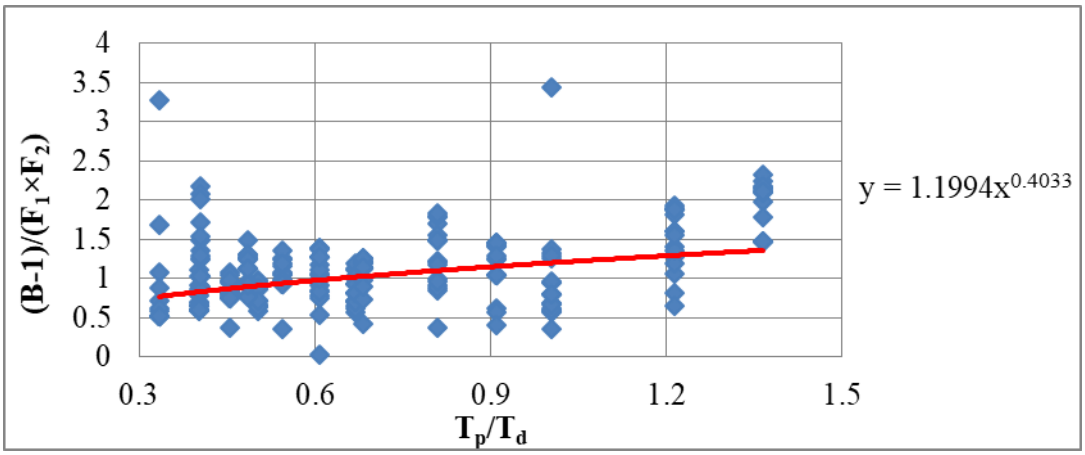

(c)

Figure 4.2. (a) *B*-1 versus ξ_e-0.05 plot and minimum least square fit of the data, (b) (*B*-1)/F_1 versus mA_p/Q_d plot and minimum least square fit of the data, (c) (*B*-1)/(F_1×F_2) versus T_p/T_d plot and minimum least square fit of the data

4.4. The Relationship between the Pulse Period (T_p) and Response Spectrum Second Corner Period (T_c)

Using the pulse period in the damping reduction equation is not practical since the design response spectrum is employed in the ELA of seismic isolated structures rather than any specific ground motion data. Accordingly, a relationship between the second corner period, T_c of the design response spectrum and the velocity pulse period would be an essential tool to replace T_p in the damping reduction equation by T_c. This will

facilitate the use of the proposed damping reduction equation in practical design applications.

To obtain a relationship between the velocity pulse period T_p, and the second corner period, T_c of the response spectrum, 84 NGM with FRDE are obtained from the PEER database and sorted according to their velocity pulse periods from small to large. Then, the ground motion data are grouped into 12 different sets of seven ground motions. Next, the average response spectra of the seven ground motions within each group are obtained. In addition, the average velocity pulse periods of the seven ground motions are calculated for each group. Then, the smoothed response spectra of each group of ground motions are obtained as described earlier in Chapter 2.3. The NGM that are used to obtain a relationship between the T_p and T_c are listed in Table 4.1. The acceleration response spectrum of each ground motion are shown in Fig. 4.3 (a), Fig. 4.4 (a), Fig. 4.5 (a), Fig. 4.6 (a), Fig. 4.7 (a), Fig. 4.8 (a), Fig. 4.9 (a), Fig. 4.10(a), Fig. 4.11 (a), Fig. 4.12 (a), Fig. 4.13 (a) and Fig. 4.14 (a) for each group respectively and their average spectrum and the smoothed response spectrum for each set of ground motions are shown in Fig. 4.3 (b), Fig. 4.4 (b), Fig. 4.5 (b), Fig. 4.6 (b), Fig. 4.7 (b), Fig. 4.8 (b), Fig. 4.9 (b), Fig. 4.10(b), Fig. 4.11 (b), Fig. 4.12 (b), Fig. 4.13 (b) and Fig. 4.14 (b) for each group respectively

Table 4.1. *NGM used to obtain a relationship between the Tp and Tc*

Soil Type	Earthquake	Station	Mw	R (km)	A_p (g)	T_p (s)	Avg. T_p (s)
Group 1	Coalinga-07	Coalinga-14th & Elm (Old CHP)	5.2	10.9	0.73	0.40	0.62
	Northridge-01	Pacoima Dam (downstr)	6.7	7.0	0.50	0.50	
	Parkfield-02_ CA	Parkfield - Cholame 3E	6.0	5.6	0.52	0.52	
	Coalinga-05	Oil City	5.8	8.5	0.87	0.69	
	Parkfield-02_ CA	Parkfield - Cholame 4W	6.0	4.2	0.58	0.70	
	Northridge-01	Pacoima Kagel Canyon	6.7	7.3	0.30	0.73	
	Nahanni- Canada	Site 2	6.8	4.9	0.47	0.81	
Group 2	Parkfield-02_ CA	Slack Canyon	6.0	3.0	0.21	0.85	0.91
	San Salvador	Geotech Investig Center	5.8	6.3	0.85	0.86	
	Duzce_ Turkey	Bolu	7.1	12.0	0.75	0.88	
	Northridge-01	Pacoima Dam (upper left)	6.7	7.0	1.39	0.90	
	Coalinga-05	Transmitter Hill	5.8	9.5	0.86	0.92	
	Morgan Hill	Coyote Lake Dam (SW Abut)	6.2	0.5	0.82	0.95	
	San Salvador	National Geografical Inst	5.8	7.0	0.42	1.00	

Soil Type	Earthquake	Station	Mw	R (km)	A_p (g)	T_p (s)	Avg. T_p (s)
Group 3	Chi-Chi_ Taiwan-06	TCU080	6.3	10.2	0.54	1.02	1.10
	Parkfield-02_ CA	Parkfield - Cholame 3W	6.0	3.6	0.33	1.02	
	Parkfield-02_ CA	Parkfield - Cholame 2WA	6.0	3.0	0.62	1.08	
	Mammoth Lakes-06	Long Valley Dam (Upr L Abut)	5.9	16.2	0.40	1.10	
	Parkfield-02_ CA	Parkfield - Fault Zone 9	6.0	2.9	0.15	1.13	
	Coyote Lake	Gilroy Array #3	6.7	7.4	0.25	1.16	
	Parkfield-02_ CA	Parkfield - Fault Zone 1	6.0	2.5	0.61	1.19	
Group 4	Loma Prieta	Gilroy Array #1	6.9	9.6	0.43	1.20	1.23
	Coyote Lake	Gilroy Array #6	5.7	3.1	0.45	1.20	
	Morgan Hill	Gilroy Array #6	6.2	9.9	0.24	1.20	
	Northridge-01	Rinaldi Receiving Sta	6.7	6.5	0.87	1.20	
	Parkfield-02_ CA	Parkfield- Eades	6.0	2.9	0.32	1.22	
	Northridge-01	Pardee - SCE	6.7	7.5	0.56	1.23	
	Parkfield-02_ CA	Parkfield - Cholame 1E	6.0	3.0	0.44	1.33	
Group 5	Coyote Lake	Gilroy Array #4	5.7	5.7	0.23	1.35	1.44
	Chi-Chi- Taiwan	CHY035	7.6	12.7	0.26	1.40	
	Westmorland	Westmorland Fire Sta	5.9	6.5	0.42	1.40	
	N. Palm Springs	North Palm Springs	6.1	4.0	0.67	1.40	
	Coyote Lake	Gilroy Array #2	5.7	9.0	0.19	1.46	
	Loma Prieta	Gilroy Array #3	6.9	12.8	0.53	1.50	
	Tottori_ Japan	TTR008	6.6	6.9	0.32	1.54	

Soil Type	Earthquake	Station	Mw	R (km)	A_p (g)	T_p (s)	Avg. T_p (s)
Group 6	San Fernando	Pacoima Dam (upper left abut)	6.6	1.8	1.45	1.60	1.74
	Northridge-01	LA Dam	6.7	5.9	0.60	1.70	
	Loma Prieta	Gilroy Array #2	6.9	11.1	0.41	1.70	
	Irpinia_ Italy-01	Bagnoli Irpinio	6.9	8.2	0.13	1.71	
	Loma Prieta	Gilroy - Gavilan Coll.	6.9	10.0	0.29	1.80	
	Loma Prieta	Gilroy - Historic Bldg.	6.9	11.0	0.25	1.80	
	Loma Prieta	Saratoga - W Valley Coll.	6.9	9.3	0.40	1.90	
Group 7	Cape Mendocino	Centerville Beach_ Naval Fac	7.0	18.3	0.32	1.97	2.24
	Superstition Hills-02	Gilroy Array #6	6.5	18.5	0.11	2.13	
	Northridge-01	Kornbloom Road (temp)	6.7	5.9	0.74	2.20	
	Imperial Valley-06	Agrarias	6.5	0.7	0.31	2.30	
	Superstition Hills-02	Parachute Test Site	6.5	0.9	0.42	2.30	
	Imperial Valley-06	Aeropuerto Mexicali	6.5	0.3	0.36	2.40	
	Superstition Hills-02	El Centro Imp. Co. Cent	6.5	18.2	0.31	2.40	
Group 8	Northridge-01	Newhall - W Pico Canyon Rd.	6.7	5.5	0.42	2.40	2.71
	Chi-Chi_ Taiwan-04	CHY074	6.2	6.2	0.34	2.44	
	Chi-Chi_ Taiwan	CHY006	7.6	9.8	0.31	2.60	
	Erzican- Turkey	Erzincan	6.7	4.4	0.49	2.70	
	Kobe_ Japan	Port Island (0 m)	6.9	3.3	0.35	2.83	
	Cape Mendocino	Petrolia	7.0	8.2	0.62	3.00	
	Loma Prieta	LGPC	6.9	3.9	1.05	3.00	

Soil Type	Earthquake	Station	Mw	R (km)	A_p (g)	T_p (s)	Avg. T_p (s)
Group 9	Northridge-01	Sylmar - Olive View Med FF	6.7	5.3	0.74	3.10	3.28
	Northridge-01	Jensen Filter Plant Adm. Buil.	6.7	5.4	0.41	3.16	
	Denali_ Alaska	TAPS Pump Station #10	7.9	2.7	0.33	3.16	
	Irpinia_ Italy-01	Sturno (STN)	6.9	10.8	0.23	3.27	
	Imperial Valley-06	EC Meloland Overpass FF .	6.5	0.1	0.38	3.30	
	Northridge-01	Jensen Filter Plant Generator	6.7	5.4	0.52	3.50	
	Northridge-01	Sylmar-Converter Sta East	6.7	5.2	0.84	3.50	
Group 10	Imperial Valley-06	El Centro Array #6	6.5	1.4	0.44	3.80	4.19
	Imperial Valley-06	El Centro Array #5	6.5	4.0	0.38	4.00	
	Chi-Chi_Taiwan-06	TCU078	6.3	11.5	0.39	4.15	
	Imperial Valley-06	El Centro Array #7	6.5	0.6	0.46	4.20	
	Westmorland	Parachute Test Site	5.9	16.7	0.23	4.39	
	Imperial Valley-06	Brawley Airport	6.5	10.4	0.17	4.40	
	Imperial Valley-06	EC County Center FF	6.5	7.3	0.21	4.42	

Soil Type	Earthquake	Station	Mw	R (km)	A_p (g)	T_p (s)	Avg. T_p (s)
Group 11	Loma Prieta	Saratoga - Aloha Ave	6.9	5.3	0.36	4.50	4.65
	Imperial Valley-06	El Centro Array #3	6.5	5.4	0.27	4.50	
	Imperial Valley-06	El Centro Array #10	6.5	2.7	0.17	4.52	
	Imperial Valley-06	El Centro Array #4	6.5	10.8	0.36	4.60	
	Chi-Chi_ Taiwan	TCU076.	7.6	0.1	0.34	4.73	
	Imperial Valley-06	Holtville Post Office	6.5	5.4	0.26	4.80	
	Cape Mendocino	Cape Mendocino	7.0	5.2	1.30	4.90	
Group 12	Kocaeli_ Turkey	Yarimca	7.5	1.4	0.23	4.95	5.35
	Landers	Lucerne	7.3	4.0	0.73	5.10	
	Chi-Chi_ Taiwan	CHY101	7.6	11.5	0.34	5.34	
	Cape Mendocino	Bunker Hill FAA	7.0	0.6	0.18	5.36	
	Chi-Chi_ Taiwan	TCU036	7.6	16.7	0.14	5.38	
	Imperial Valley-06	El Centro Array #8	6.5	10.4	0.47	5.40	
	Imperial Valley-06	El Centro Differential Array	6.5	7.3	0.42	5.90	

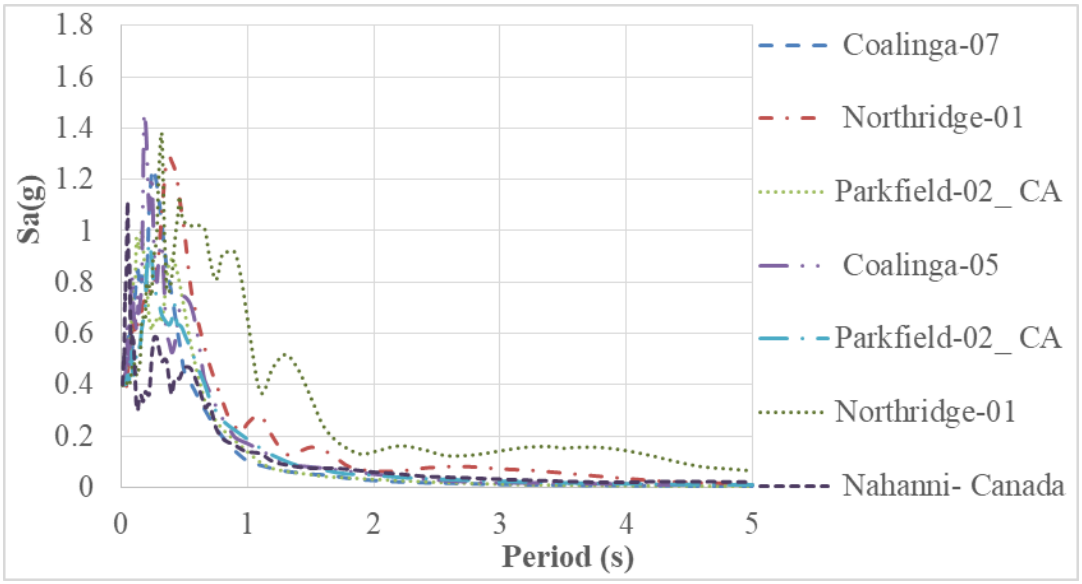

(a)

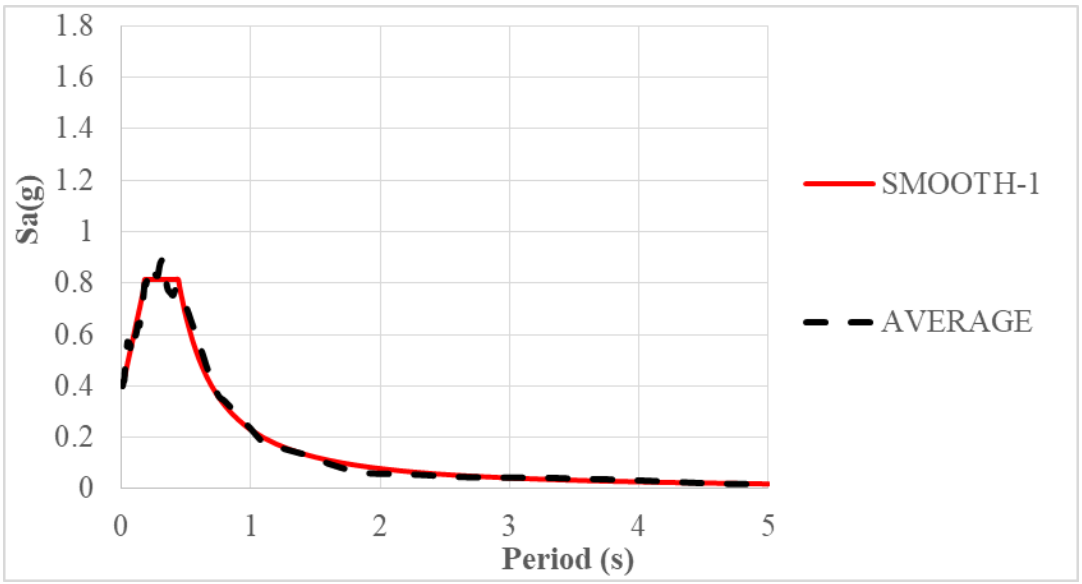

(b)

Figure 4.3. Group-1 ground motions used to obtain a relationship between the T_p and T_c (a) Response spectra (b) average and smoothed spectra

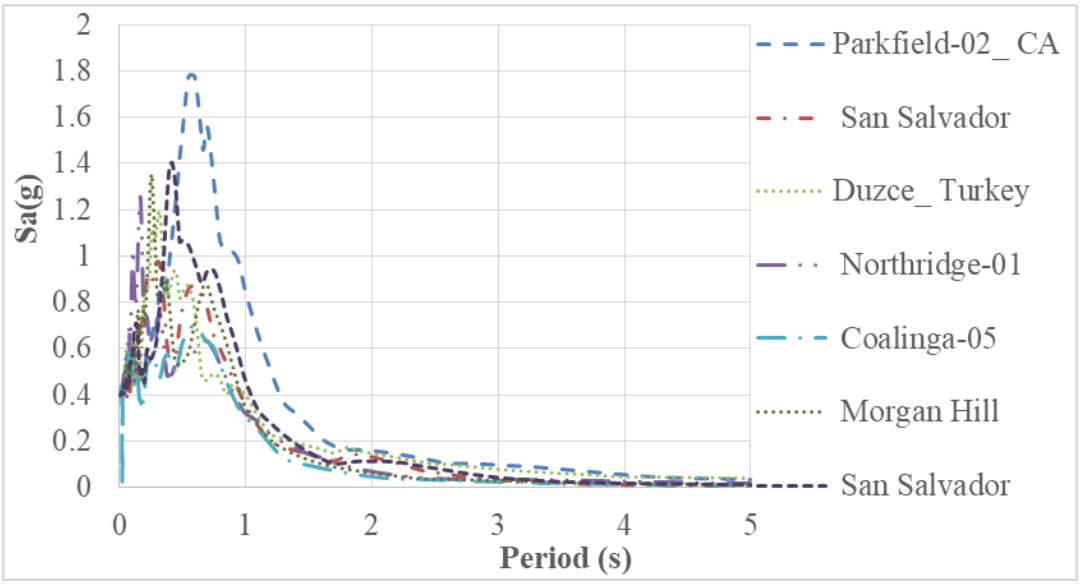

(a)

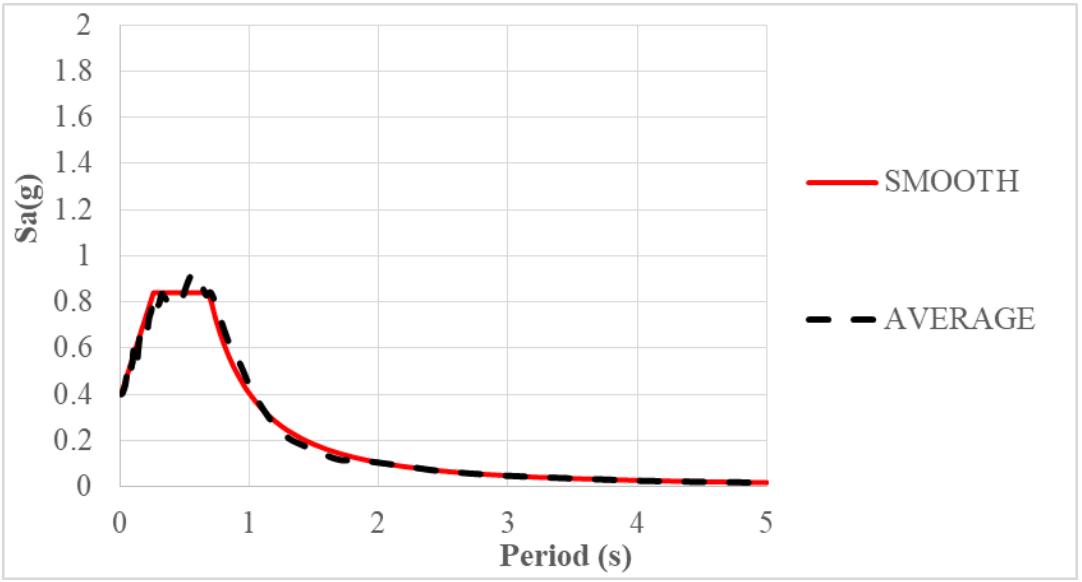

(b)

Figure 4.4. Group-2 ground motions used to obtain a relationship between the T_p and T_c (a) Response spectra (b) average and smoothed spectra

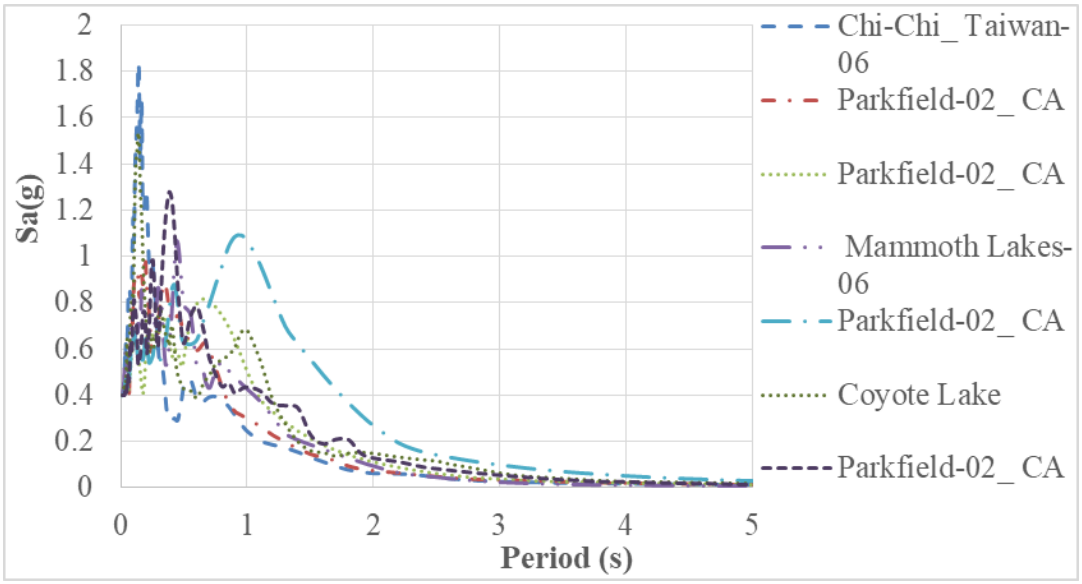

(a)

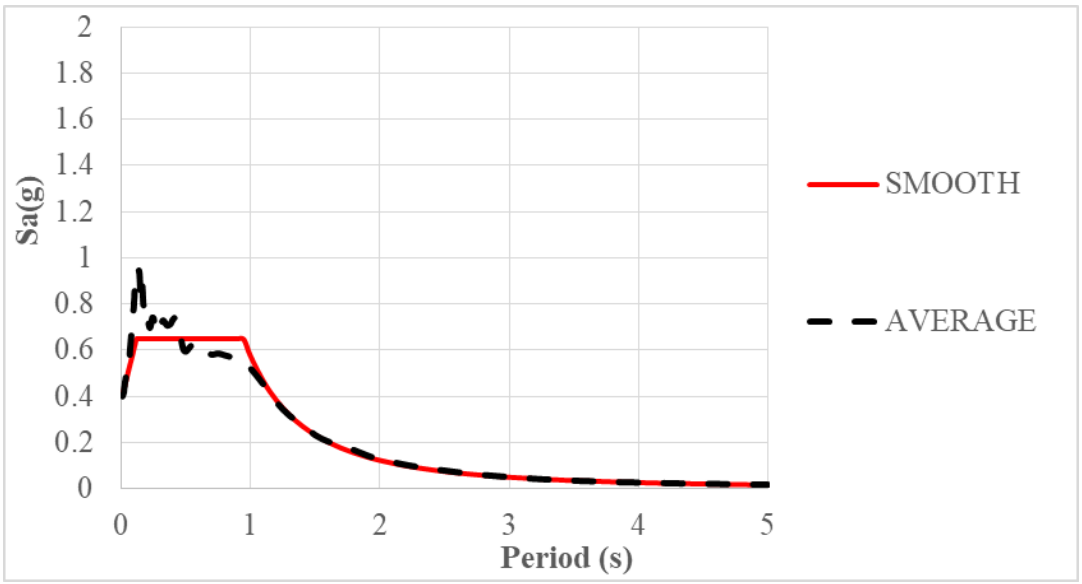

(b)

Figure 4.5. Group-3 ground motions used to obtain a relationship between the T_p and T_c (a) Response spectra (b) average and smoothed spectra

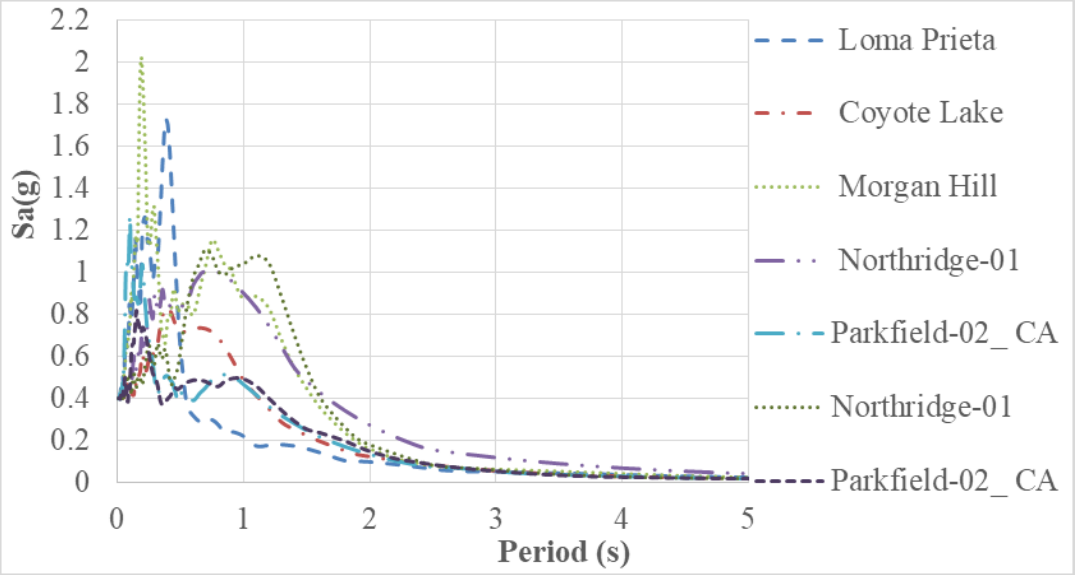

(a)

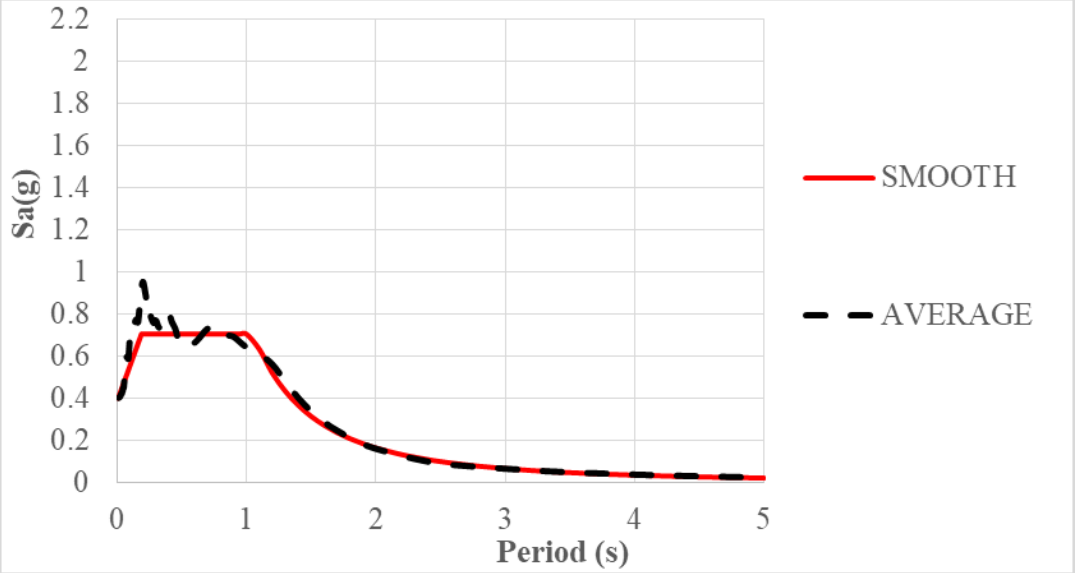

(b)

Figure 4.6. Group-4 ground motions used to obtain a relationship between the T_p and T_c (a) Response spectra (b) average and smoothed spectra

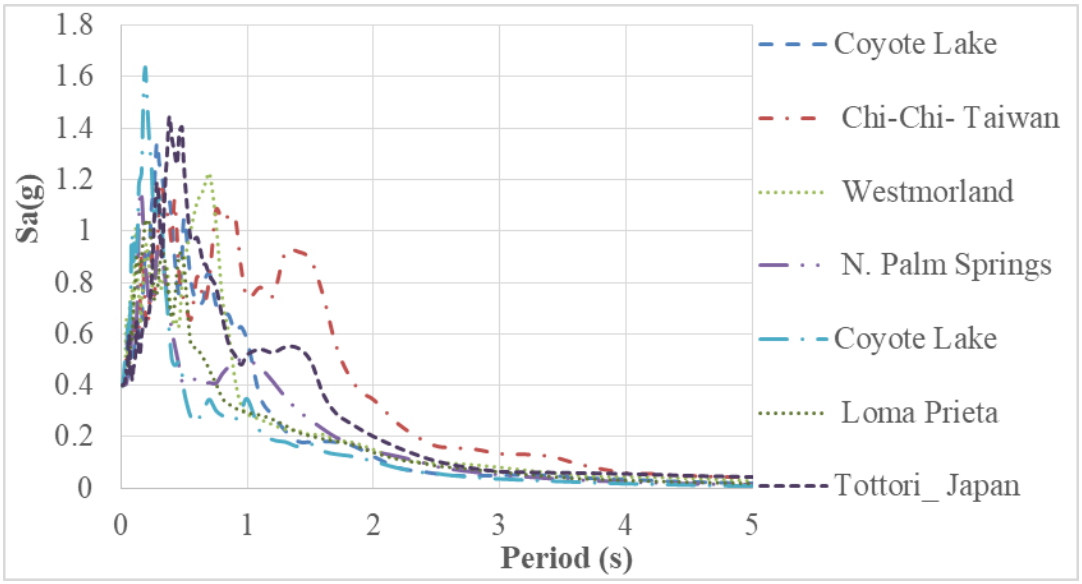

(a)

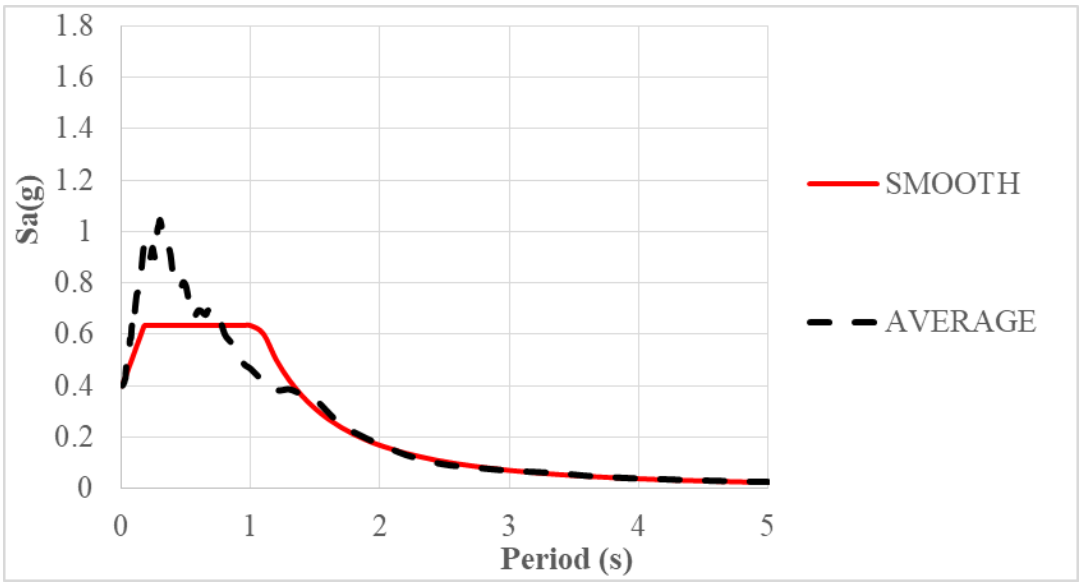

(b)

Figure 4.7. Group-5 ground motions used to obtain a relationship between the T_p and T_c (a) Response spectra (b) average and smoothed spectra

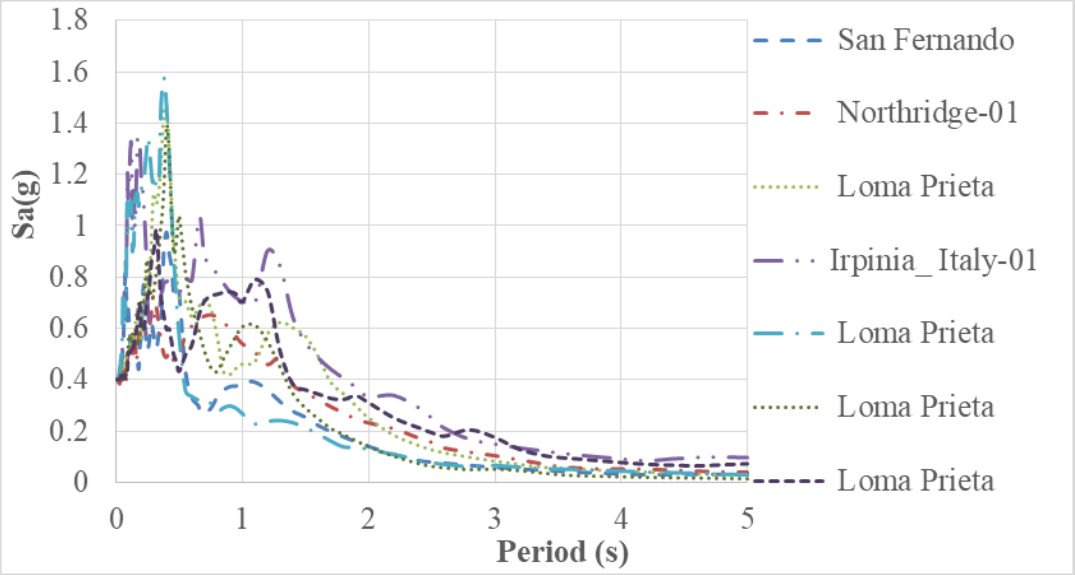

(a)

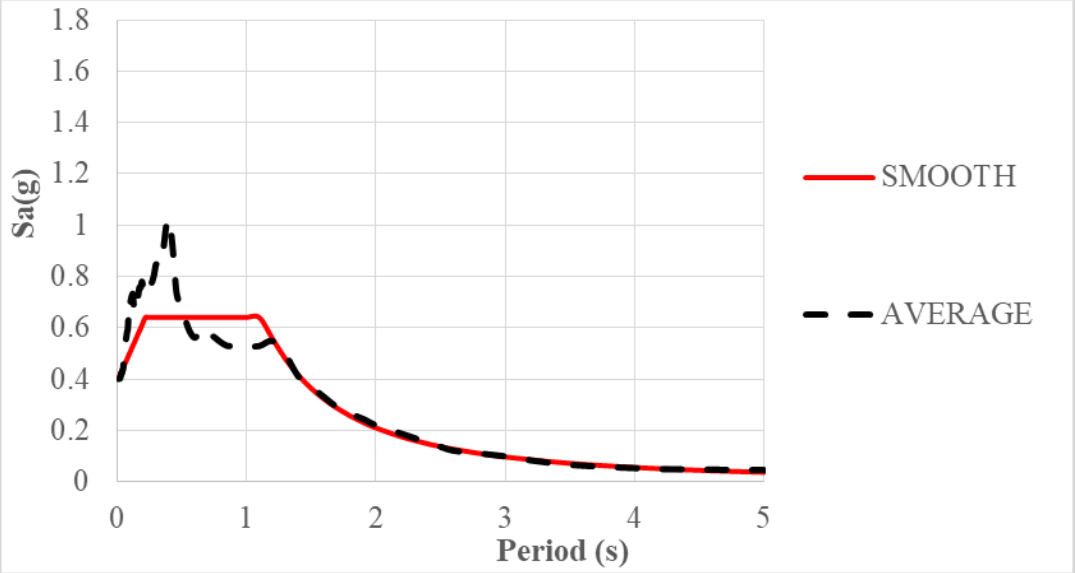

(b)

Figure 4.8. Group-6 ground motions used to obtain a relationship between the T_p and T_c (a) Response spectra (b) average and smoothed spectra

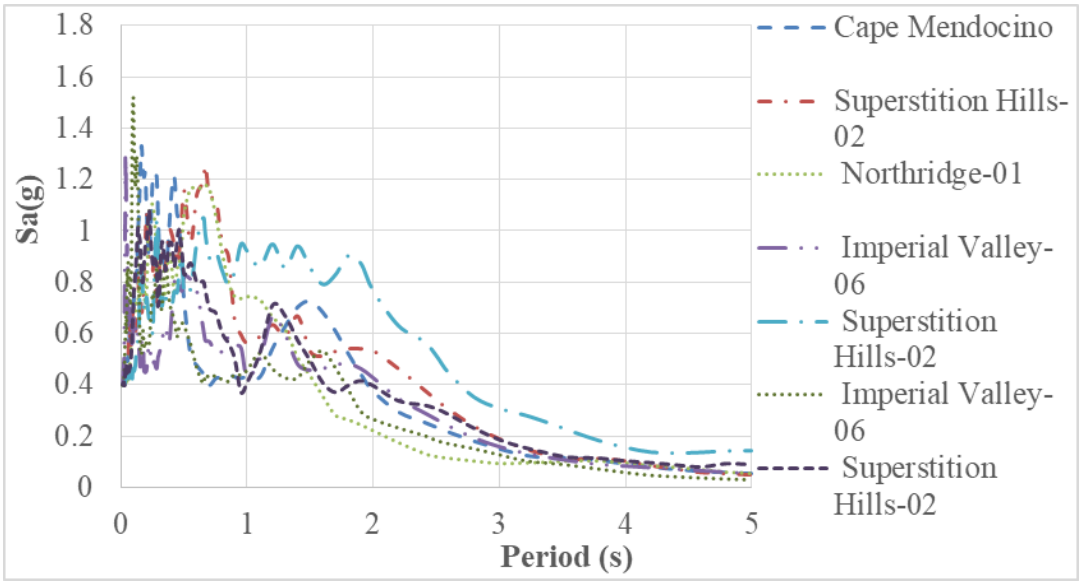

(a)

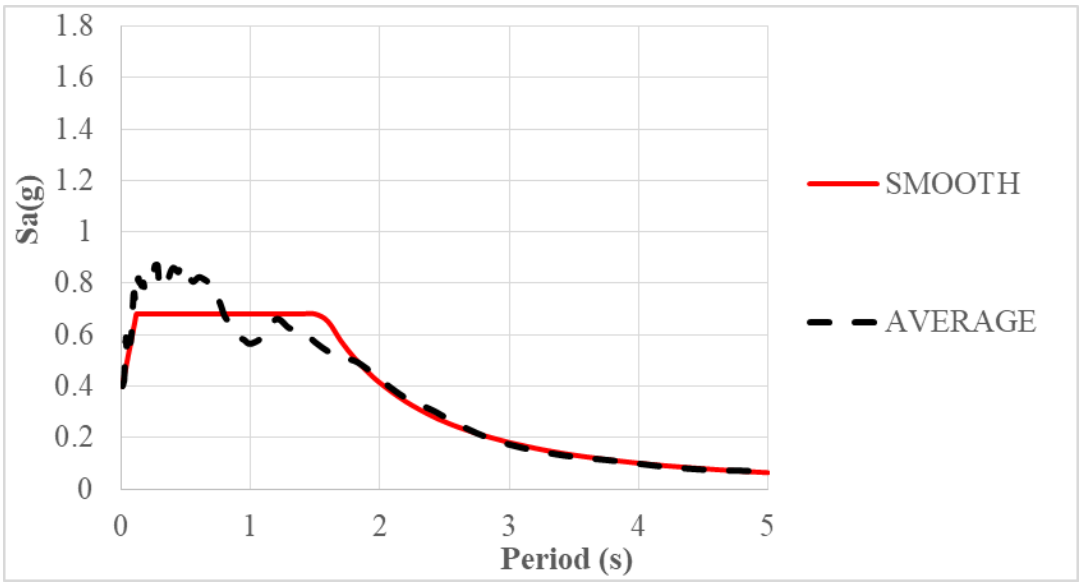

(b)

Figure 4.9. Group-7 ground motions used to obtain a relationship between the T_p and T_c (a) Response spectra (b) average and smoothed spectra

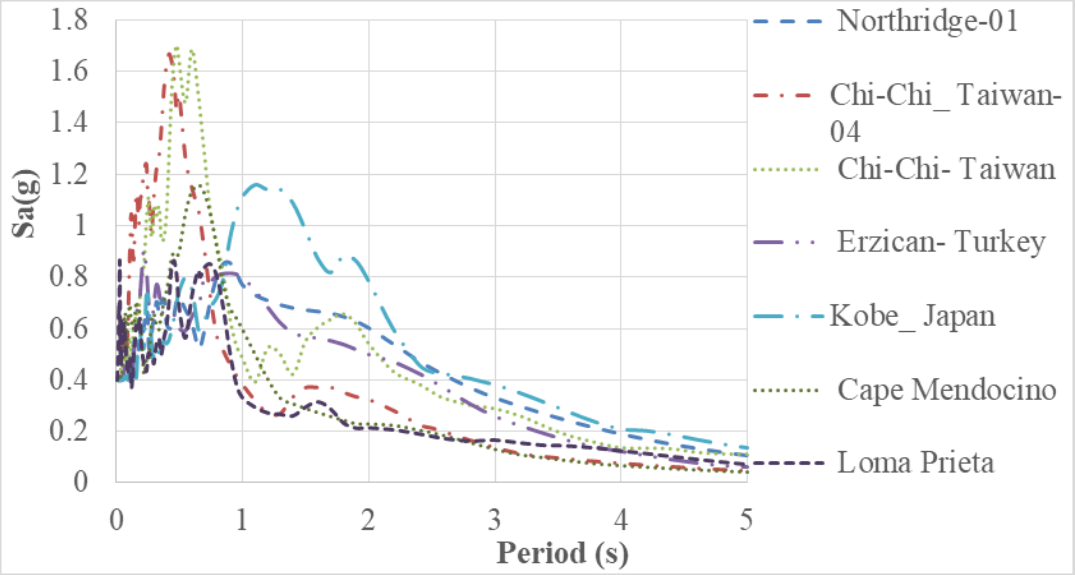

(a)

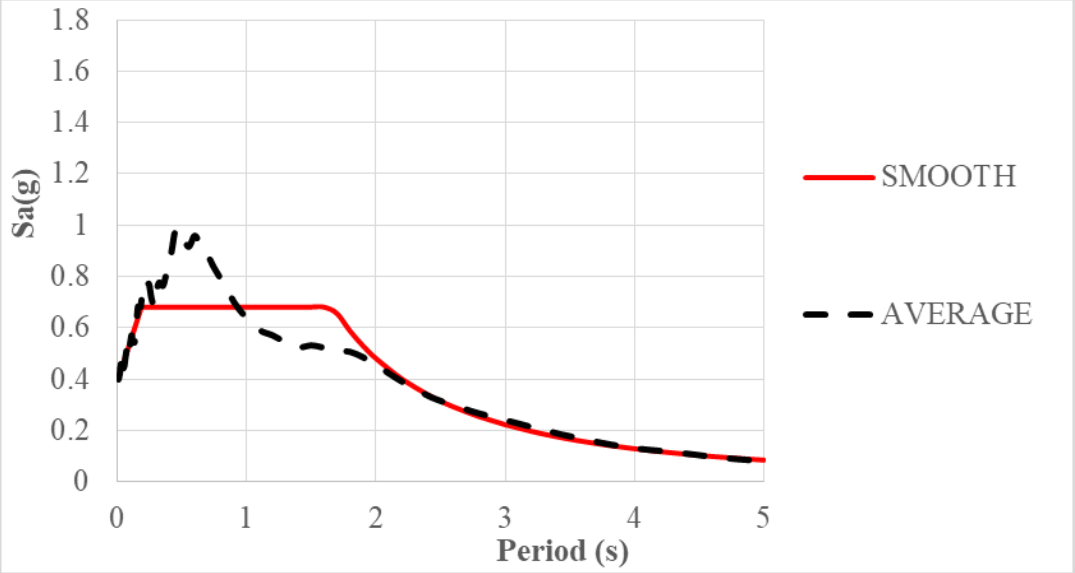

(b)

Figure 4.10. Group-8 ground motions used to obtain a relationship between the T_p and T_c (a) Response spectra (b) average and smoothed spectra

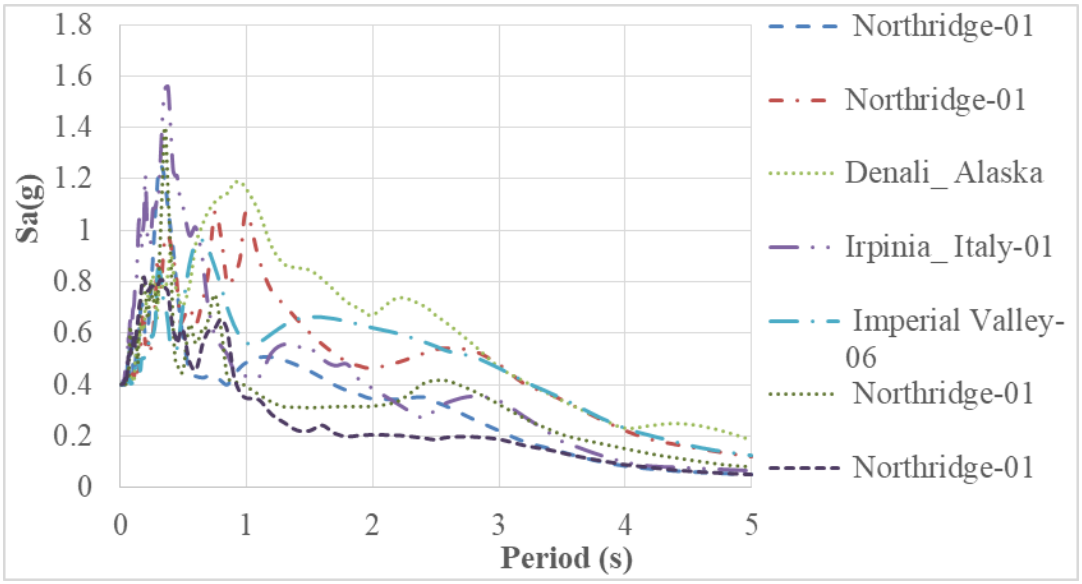

(a)

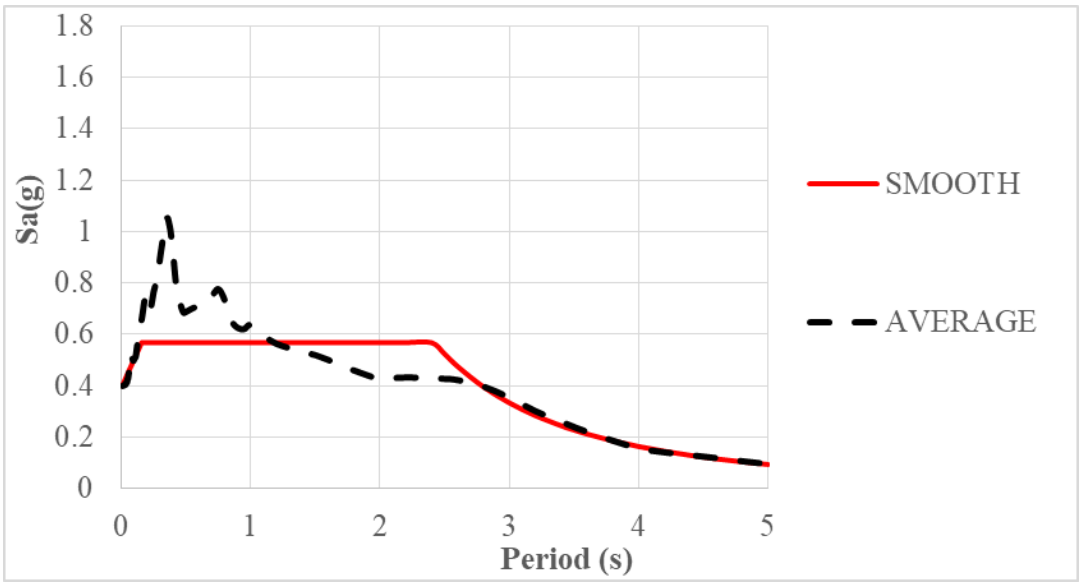

(b)

Figure 4.11. Group-9 ground motions used to obtain a relationship between the T_p and T_c (a) Response spectra (b) average and smoothed spectra

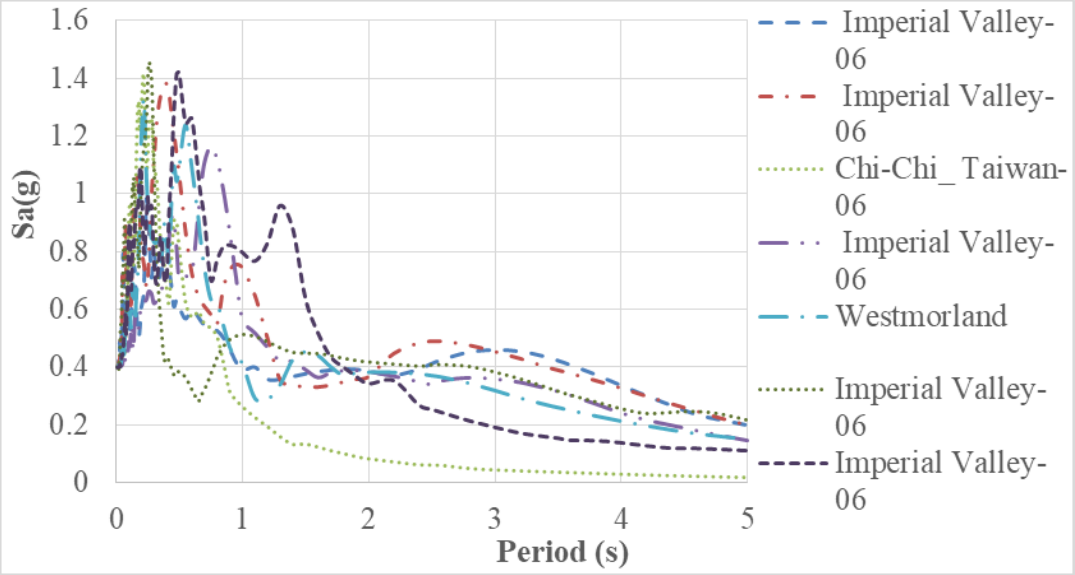

(a)

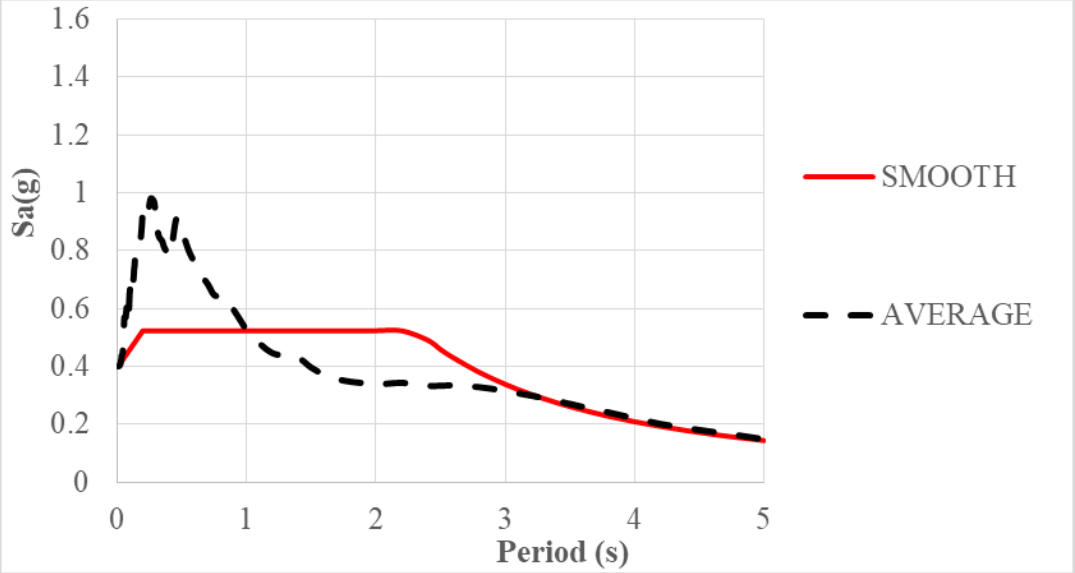

(b)

Figure 4.12. Group-10 ground motions used to obtain a relationship between the T_p and T_c (a) Response spectra (b) average and smoothed spectra

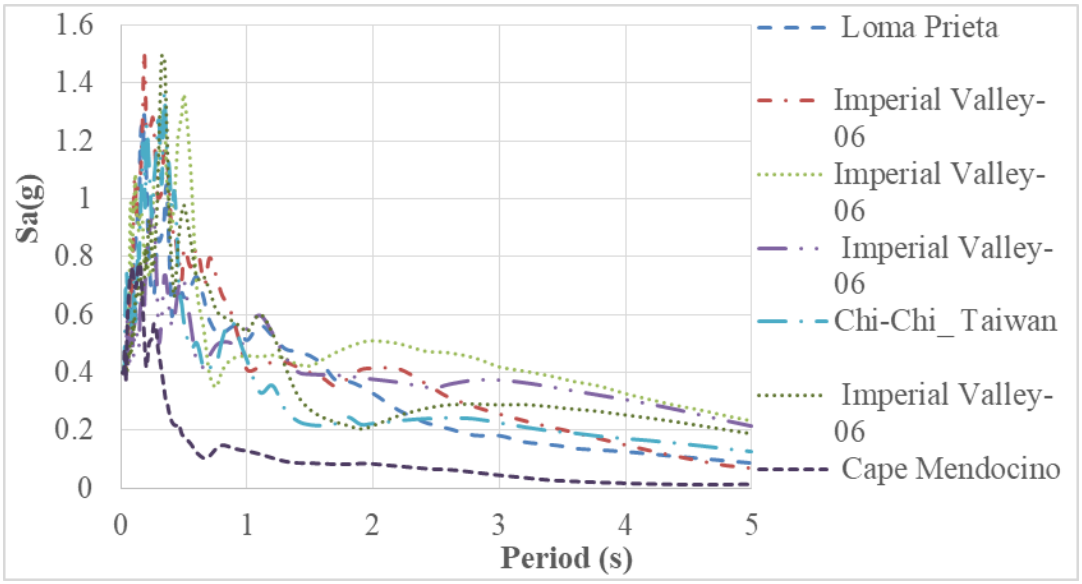

(a)

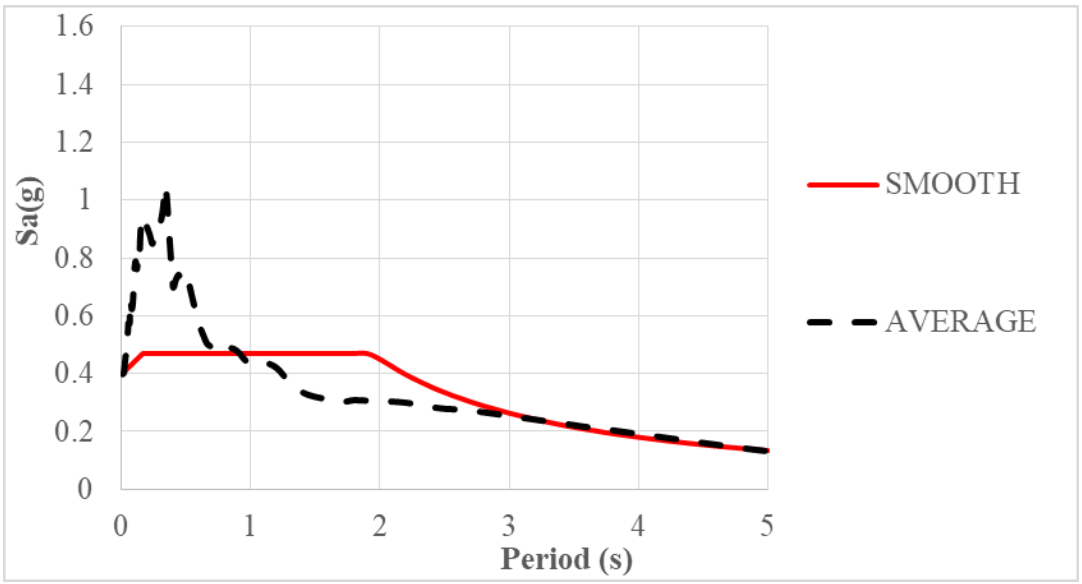

(b)

Figure 4.13. Group-11 ground motions used to obtain a relationship between the T_p and T_c (a) Response spectra (b) average and smoothed spectra

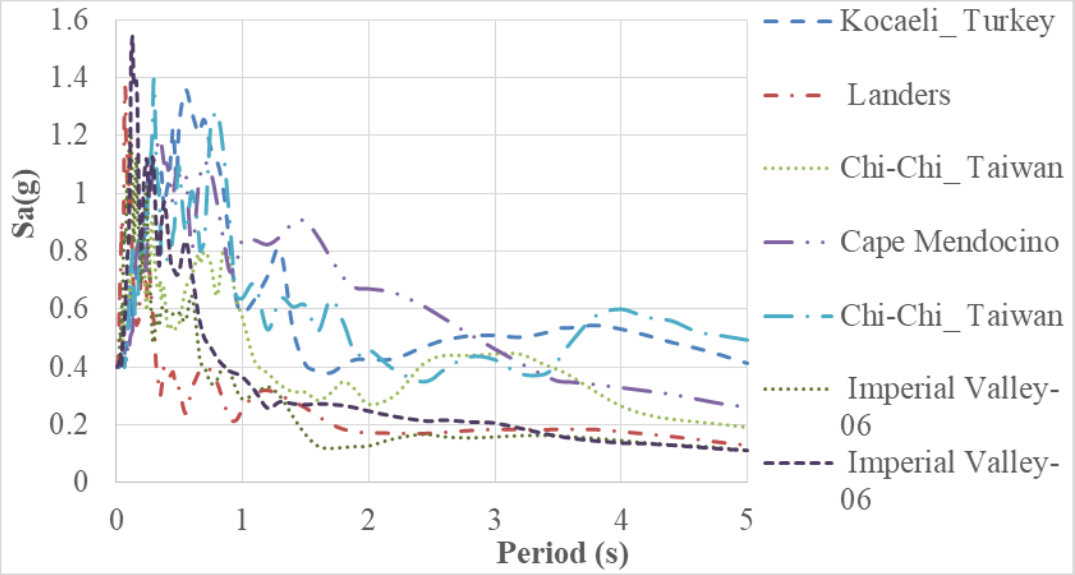

(a)

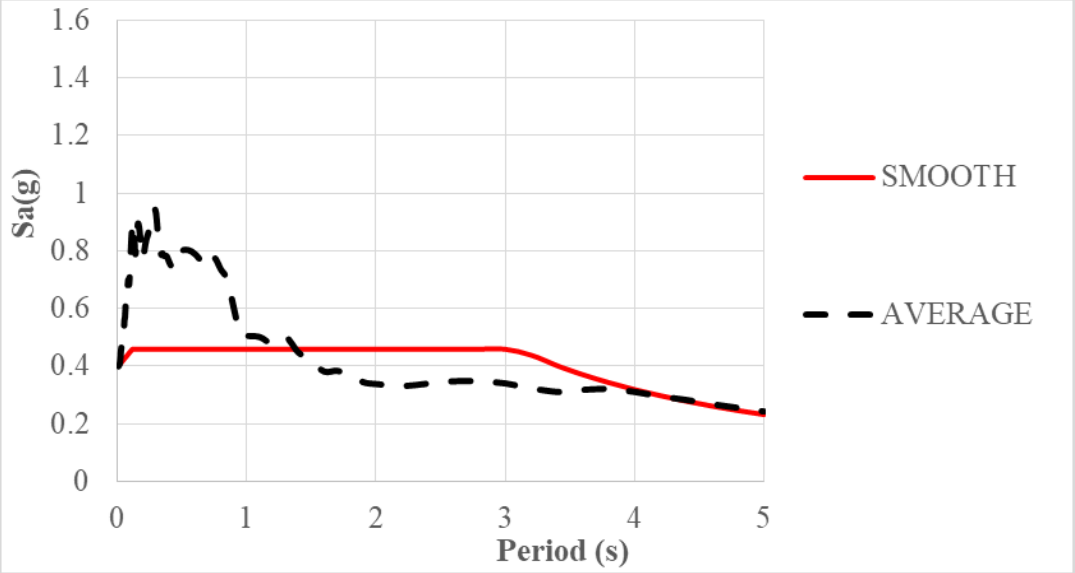

(b)

Figure 4.14. Group-12 ground motions used to obtain a relationship between the Tp and Tc (a) Response spectra (b) average and smoothed spectra

The corner periods of the smoothed response spectra and the average velocity pulse period of each group of ground motions are listed as a value in Table 4.2 and the relationship between T_c and T_p is plotted in Fig. 4.15. As observed from the figure, T_p vs. T_c relationship follows nearly a linear trend of the form $T_p=\alpha T_c$. A sensitivity analysis is conducted on the value of α by assigning values ranging between 1.4 and 2.0 (Fig. 4.15). It is found that while a value of $\alpha=1.7$ effectively simulates the trend of the data, it also results in an equation with more rounded-off coefficients.

Finally, 1.7 T_c is inserted in place of T_p in Equation.4.7 and the proposed damping reduction equation takes the following final form:

$$B = 1 + 3 \times (\xi_e - 0.05)^{0.85}\left(\frac{Q_d}{mA_p}\right)^{0.25}\left(\frac{T_c}{T_d}\right)^{0.40} \qquad \text{(Eq. 4.8)}$$

Table 4.2. *Second corner periods of the smoothed response spectra and the average velocity pulse period of each group*

Group #	**T_c (s)**	**Avg. T_p (s)**
1	0.44	0.62
2	0.67	0.91
3	0.90	1.10
4	1.10	1.23
5	1.00	1.44
6	1.10	1.74
7	1.50	2.24
8	1.60	2.71
9	2.40	3.28
10	2.20	4.19
11	1.90	4.65
12	3.00	5.35

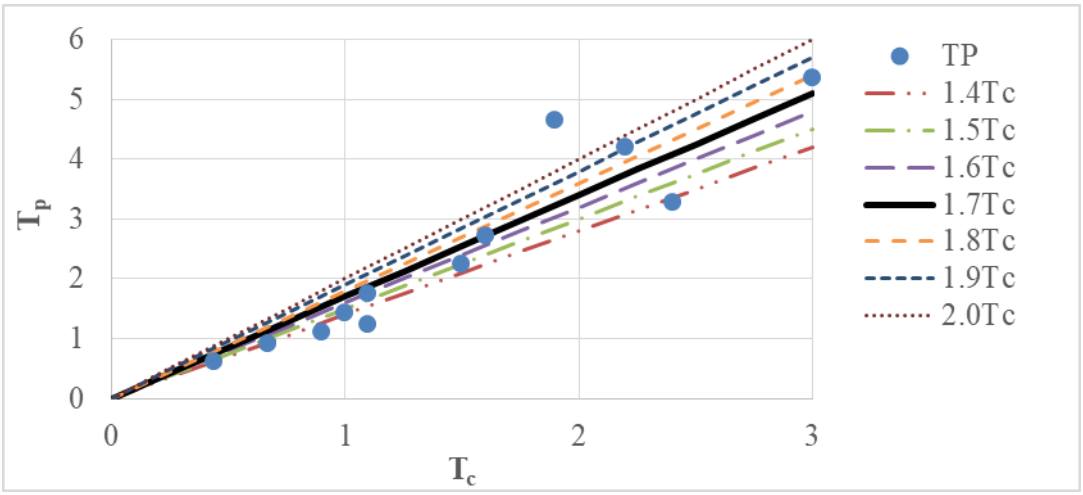

Figure 4.15. The relationship between Tc and Tp

CHAPTER 5

VERIFICATION OF THE PROPOSED DAMPING REDUCTION EQUATION

5.1. Verification of the Improved Damping Reduction Equation

In this section, the impact of the proposed damping reduction equation on the accuracy of the ELA results is investigated using the 29 NGM used in the development of the proposed equation and nine additional NGM tabulated in Table 2.2, which are used in the independent verification of the proposed equation. The first verification is performed using the data employed in the development of the proposed equation. For this purpose, first, 375 ELA of seismic isolated structures considered in this study are performed using the smoothed average response spectrum of the 29 NGM for each site soil classification (three different response spectra for soil classifications A&B, C and D) and the displacements, Δ_{ELA}, are obtained. The ELA are conducted using the damping reduction equation proposed in this study as well as those proposed by AASHTO (2014), Priestley et al. (2007) and Hubbard & Mavroeidis (2011). This resulted in 1500 (4×375=1500) ELA cases. Next, 3625 (875 / 7 + 1375 / 11 + 1375 / 11 = 375) NLTHA results of the seismic isolated structures considered in the development of the proposed equation are used to obtain the averages of the displacements, Δ_{NLTHA}, from each set of ground motions for each site soil classification A&B, C and D. This resulted in 375 NLTHA displacements. Then, the ratio of the displacements obtained from the ELA to those from NLTHA (Δ_{ELA}/ Δ_{NLTHA}) are calculated and the average of the calculated Δ_{ELA}/ Δ_{NLTHA} ratios are plotted in a bar-chart form (GMD: ground motions used in the development of the proposed equation) in Fig. 5.1. In the figure, each bar chart represents the average of the $\Delta_{ELA}/\Delta_{NLTHA}$ ratios for each one of the damping reduction equations, namely; AASHTO (2014), Priestley et al. (2007), Hubbard & Mavroeidis (2011) and the proposed equation. Each one of the Figs. 5.1. (a), (b), (c) and (d) shows the average

of the $\Delta_{ELA}/\Delta_{NLTHA}$ ratios for site soil classifications A&B, C, D and average of all the $\Delta_{ELA}/\Delta_{NLTHA}$ ratios regardless of the site soil classification. In the figure, the flat line represents a perfect match between the ELA and NLTHA where $\Delta_{ELA}/\Delta_{NLTHA}$=1.0. A $\Delta_{ELA}/\Delta_{NLTHA}$ ratio larger than 1.0 indicates a conservative estimate of the actual nonlinear displacement via ELA and the opposite is true for ratios smaller than 1.0

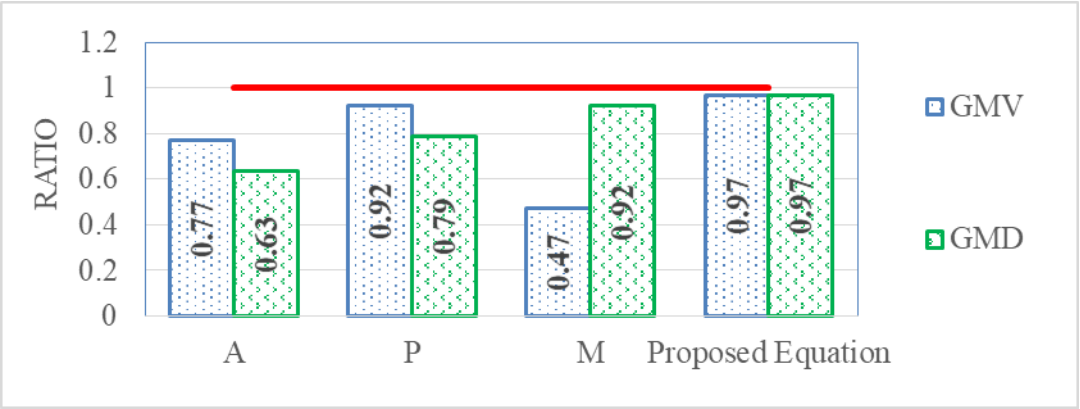

(a)

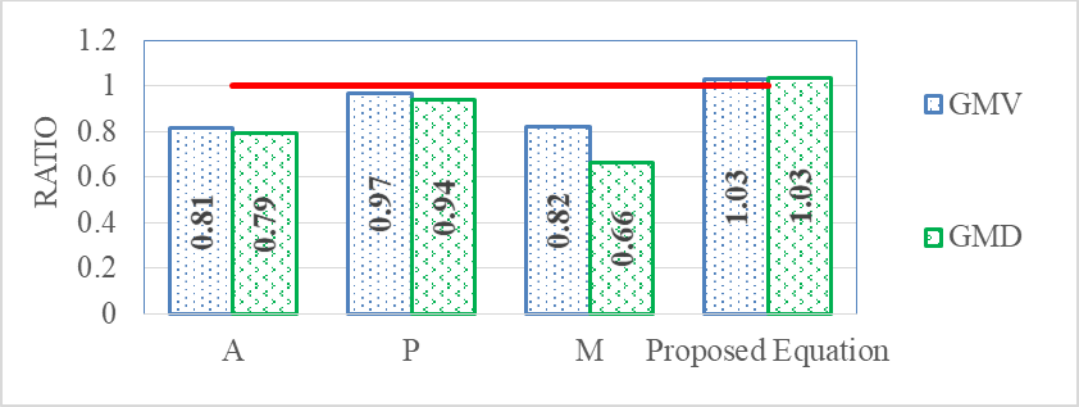

(b)

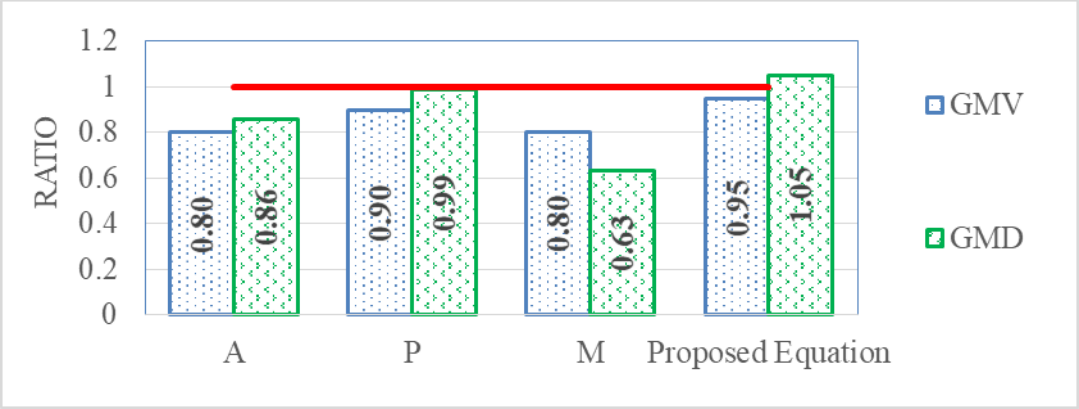

(c)

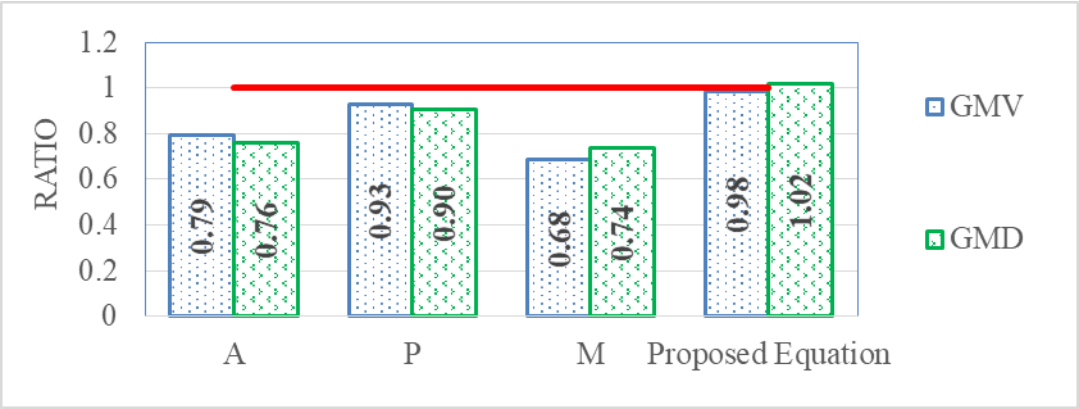

(d)

Figure 5.1. Ratio of displacements obtained from ELA to those obtained from NLTHA for site soil classifications (a) A&B, (b) C, (c) D, (d) Average from all site soil classifications. GMV= Ground motion used in the verification, GMD=Ground motions used in the development of the equation. A=AASHTO (2014), P=Priestley et al. (2007), M=Hubbard & Mavroeidis (2011), Proposed Equation= Proposed damping reduction equation.

As shown in Fig. 5.1, (a), (b) and (c) using the proposed damping reduction equation in ELA gives a consistently better estimate of the actual nonlinear responses compared to other equations for all the site soil classifications. This is expected as the proposed equation contain more variables representing the properties of the seismic isolated structures as well as the ground motion (or spectrum) while it is simple enough to be employed in practice. Fig. 5.1 (d) reveals that ELA results obtained using the proposed damping reduction equation estimates the actual nonlinear responses on the average with +/- 2% accuracy for all the cases considered in the analyses regardless of the site

soil classification. On the other hand, although the damping reduction equation proposed by Priestley et al. (2007) produces a reasonably good estimate of the actual nonlinear responses for site soil classifications C and D, it underestimates the actual nonlinear responses by as much as 21% for site soil classifications A&B. The ELA results obtained using the equations proposed by AASHTO (2014) and Hubbard & Mavroeidis (2011) on the other hand, severely underestimates the actual nonlinear responses for all the site soil classifications.

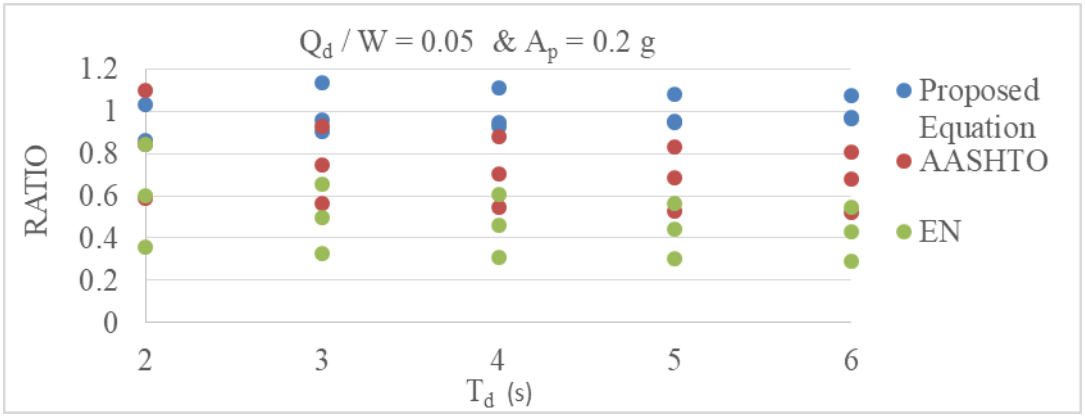

(a)

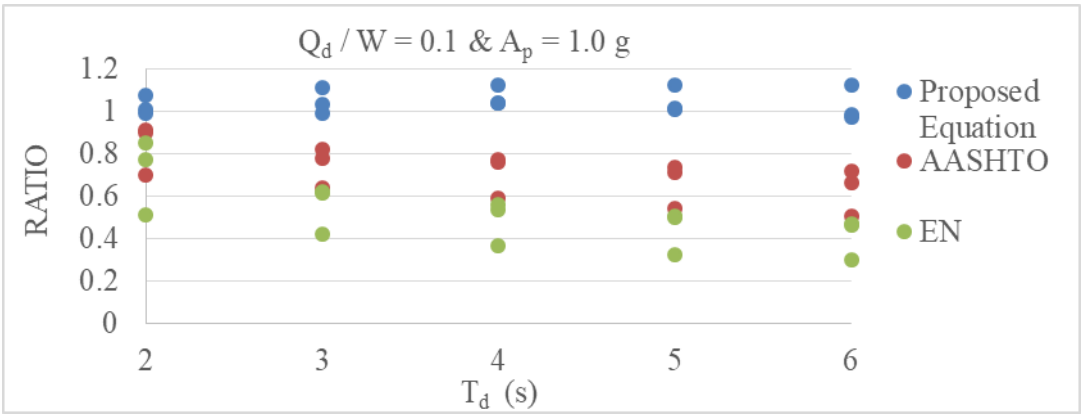

(b)

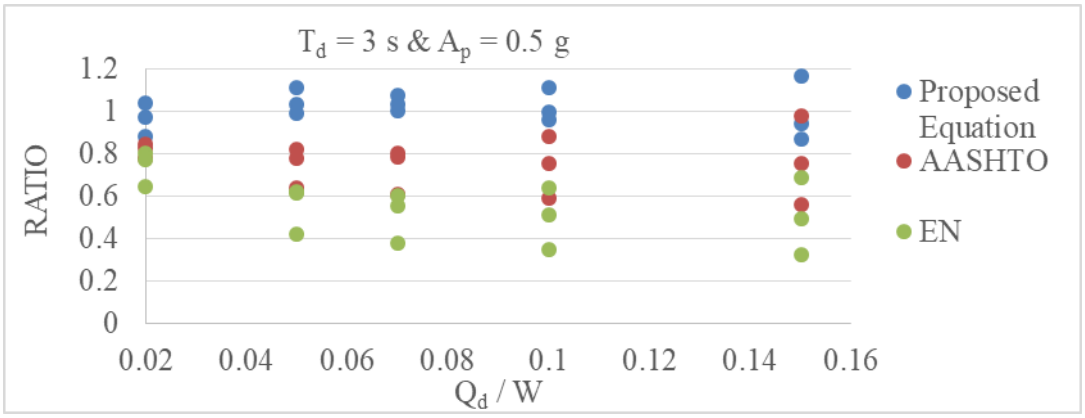
T_d = 3 s & A_p = 0.5 g
RATIO
1.2
1
0.8
0.6
0.4
0.2
0
0.02
0.04
0.06
0.08
0.1
0.12
0.14
0.16
Q_d / W
Proposed Equation
AASHTO
EN

(c)

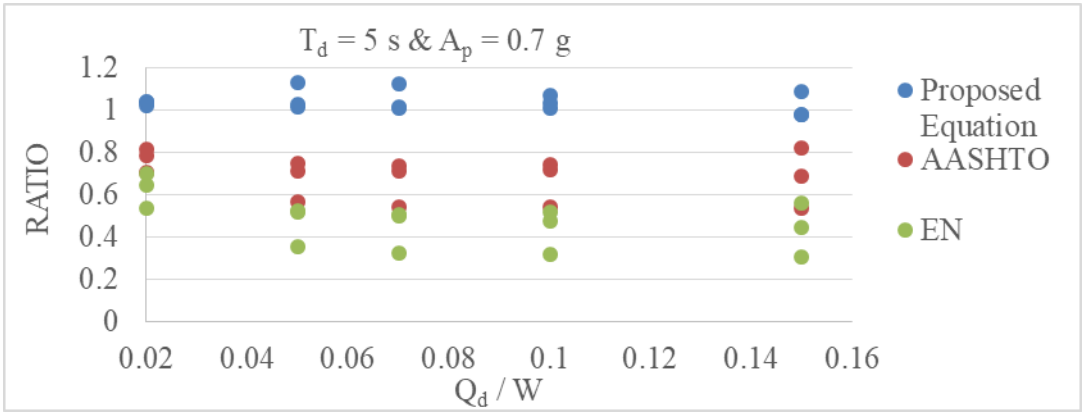
T_d = 5 s & A_p = 0.7 g
RATIO
1.2
1
0.8
0.6
0.4
0.2
0
0.02
0.04
0.06
0.08
0.1
0.12
0.14
0.16
Q_d / W
Proposed Equation
AASHTO
EN

(d)

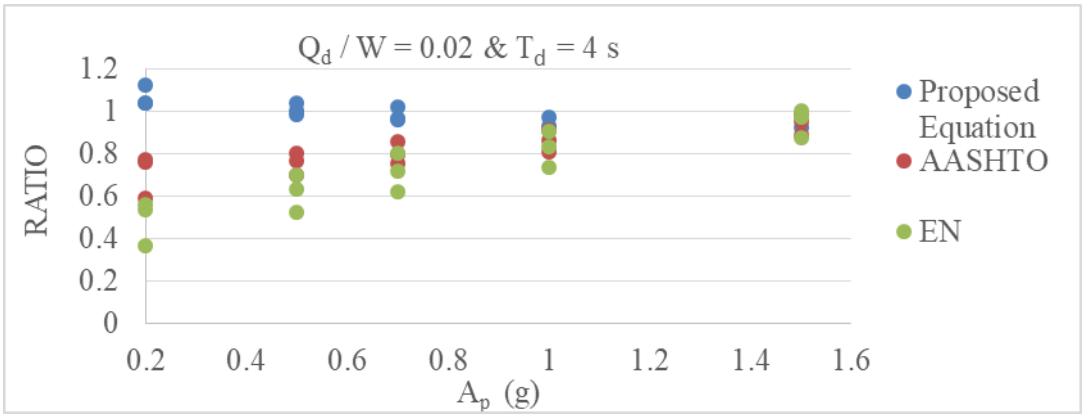
Q_d / W = 0.02 & T_d = 4 s
RATIO
1.2
1
0.8
0.6
0.4
0.2
0
0.2
0.4
0.6
0.8
1
1.2
1.4
1.6
A_p (g)
Proposed Equation
AASHTO
EN

(e)

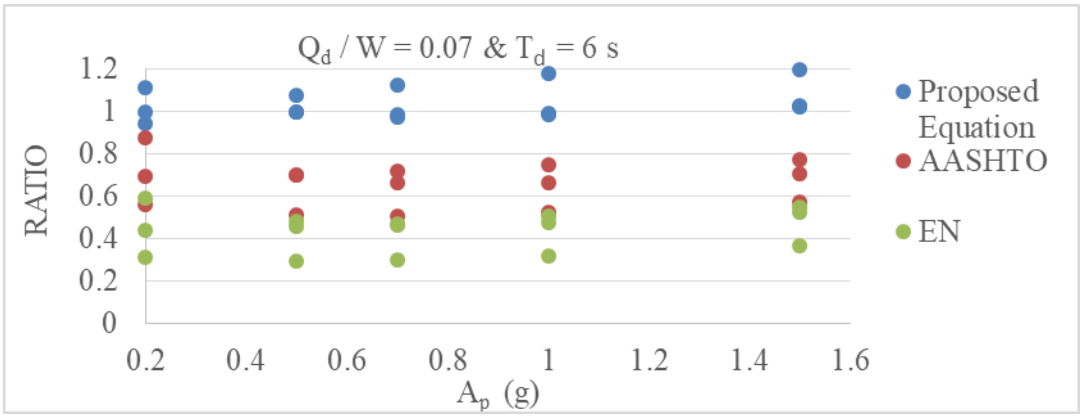

(f)

Figure 5.2. Ratio of displacements obtained from ELA by using the proposed damping reduction equation and proposed by international design codes to those obtained from NLTHA for some constants values (a) Q_d /W = 0.05 & A_p = 0.2g, (b) Q_d /W = 0.1 & A_p = 1.0 g, (c) T_d = 3 s & A_p = 0.5 g, (d) T_d = 5 s & A_p = 0.7 g, (e) Q_d /W = 0.02 & T_d = 4 s, (f) Q_d /W = 0.07 kN & T_d = 6 s

In addition, as shown in Fig. 5.2, (a), (b), (c), (d), (e), (f), using the proposed damping reduction equation in ELA gives a consistently better estimate of the actual nonlinear responses compared to equations proposed by international design codes for different parameters.

Moreover, dispersion analyses are performed for the verification analyses cases to quantify the dispersion of the error of the $\Delta_{ELA}/\Delta_{NLTHA}$ ratios as represented by equation 5.1.

$$d = \left| \frac{\frac{\Delta_{ELA}}{\Delta_{NLTHA}} - 1}{\frac{\Delta_{ELA}}{\Delta_{NLTHA}}} \right| \qquad \text{(Eq. 5.1)}$$

The dispersion analyses results are plotted in Fig. 5.2 as functions of the dimensionless terms mA_p/Q_d. Fig. 5.2 compares the dispersion of the $\Delta_{ELA}/\Delta_{NLTHA}$ data for the proposed damping reduction equation and those proposed by AASHTO (2014), Priestley et al. (2007) and Hubbard & Mavroeidis (2011). As observed from the figure the dispersion of the data for the proposed damping reduction equation is smaller than those of the other equations considered in this study. , The maximum dispersion values are 1.04, 0.69, 3.56 and 0.45 for the damping reduction equations of AASHTO (2014),

Priestley et al. (2007), Hubbard & Mavroeidis (2011) and the proposed equation respectively. This indicates that the proposed damping reduction equation produces a consistently more reliable estimates of the actual nonlinear responses. The dispersion of the $\Delta_{ELA}/\Delta_{NLTHA}$ data may be due to the strong pulse type characteristics of NGM that result in a single large offset in isolator displacement where the equivalent linearization of the seismic isolated structures behavior fails to capture some response. The high frequency components of the recorded NGM superimposed on the main pulse also contributes to the dispersion of the $\Delta_{ELA}/\Delta_{NLTHA}$ data. A close inspection of the data revealed that the dispersion is mostly concentrated for effective damping values larger than 30%. This is expected since for larger damping values the estimation of pseudo displacement via ELA losses its accuracy. Consequently, it is recommended that in near-fault zones, especially for effective damping ratios larger than 30%, ELA should generally be used for the preliminary design (e.g. to size the isolators) of seismic isolated structures. For the actual design of seismic isolated structures located in near-fault zones, three-dimensional NLTHA seems more appropriate.

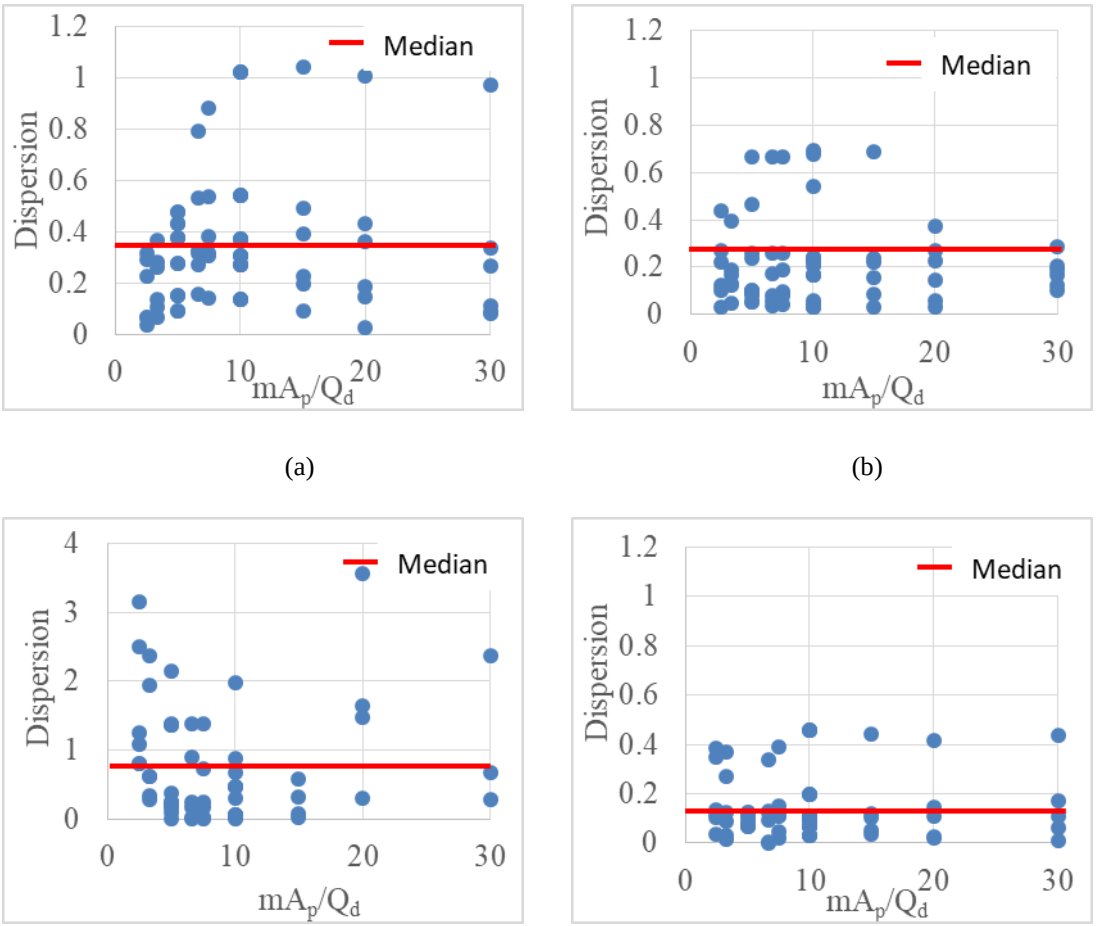

Figure 5.3. Dispersion calculated as a function of mA_p/Q_d with verification data using (a) AASHTO (2014), (b) Priestley et al. (2007), (c) Hubbard & Mavroeidis (2011) (d) Proposed damping reduction equation

CHAPTER 6

CONCLUSION

In this study, a new damping reduction equation for seismic isolated structures subjected to NGM is proposed following extensive parametric studies. The influence of the effective damping ratio (ξ_e), characteristic strength and post elastic period of isolator (Q_d, T_d), peak ground acceleration (A_p) and pulse period (T_p) of the NGM, which is expressed as a function of the second corner period (T_c) of the design response spectrum on the damping reduction factor are carefully examined and discussed. The observations drawn from this study are listed below.

i. The isolator parameters, (Q_d, T_d) and ground motion parameters (A_p , T_p or T_c) are found to affect the damping reduction factor and hence, the displacements obtained from ELA.

ii. The site soil condition is also found to affect the accuracy of the displacements obtained from ELA performed using the damping reduction equations proposed by design codes and various researchers.

iii. The analyses results revealed that the damping reduction equations proposed by the design codes and various researchers generally underestimate the actual nonlinear displacements especially for stiff soil conditions.

iv. The relationship between the pulse period of the NGM and corner period of the design response spectrum is explored as part of this research study and found to be nearly linear. Such a relationship may be used to reflect the frequency characteristics of the NGM to the design spectrum for various analysis and design applications.

v. The proposed damping reduction equation is found to yield more reasonable estimates of the actual nonlinear responses of seismic isolated structures subjected to

NGM compared to several other damping reduction equations available in the literature and international design codes regardless of the site soil conditions.

vi. Moreover, the proposed damping reduction equation is found to reduce the dispersion of the $\Delta_{ELA}/\Delta_{NLTHA}$ data compared to several other damping reduction equations available in the literature and international design codes

vii. However, although the proposed damping reduction equation improves the reliability of the ELA results for seismic isolated structures subjected to NGM, the dispersion remains relatively large, particularly for effective damping ratios larger than 30%. Therefore, it is recommended that in near-fault zones, especially for effective damping ratios larger than 30%, ELA should generally be used for the preliminary design (e.g. to size the isolators) of seismic isolated structures. For the final design, three-dimensional NLTHA seems more appropriate.

REFERENCES

American Association of State Highway and Transportation Officials _AASHTO_, 2014. Guide Specifications for Seismic Isolation Design, Washington, D.C..

European Standard _EN 15129: Anti-Seismic Devices _Brussels, 2010

ASCE 7-16 Minimum Design Loads and Associated Criteria for Buildings and Other Structures, American Society of Civil Engineers New York, NY, 2016

NEHRP National Earthquake Hazards Reduction Program NEHRP Recommended Seismic Provisions for New Buildings and Other Structures (FEMA P-750), 2009.

Buckle IC, Constantino MC, Dicleli M, Ghasemi H. Seismic Isolation of Highway Bridges. US Department of Transportation, Federal Highway Administration, New York 2006

Dicleli M, Seismic Design of Lifeline Bridge Using Hybrid Seismic Isolation. Journal of Bridge Engineering 2002; 7 (2): 94–10.

Kubin J, Kubin D, Özmen A, Sadan OB, Eroglu E, Sucuoglu H, Akkar S. Seismic Isolated Hospital Design Practice in Turkey:Erzurum Medical Campus WCEE 15, Lisbon 2012.

Rousis PC, Constantinou MC, Erdik M, Caktı E, Dicleli M, Assessment of Performance of Seismic Isolation System of Bolu Viaduct, Journal of Bridge Engineering, 8(4):182-190.

Hwang JS, Sheng LH. Effective Stiffness and Equivalent Damping of Base Isolated Bridges. Journal of Structural Engineering ASCE 1993; 119(10): 3094–101.

Hwang JS. Evaluation of ELA Methods of Bridge Isolation. Journal of Structural Engineering ASCE 1996; 122(8):972–6.

Hwang JS, Chang KC, Tsai MH. Composite Damping Ratio of Seismically Isolated Regular Bridges. Engineering Structures 1997; 19(1):52–62.

Franchin P, Monti G, Pinto PE. On the Accuracy of Simplified Methods for the Analysis of Isolated Bridges. Earthquake Engineering and Structural Dynamics 2001; 30 (3):363–82.

Dicleli M. Performance of Seismic-Isolated Bridges in Relation to Near-Fault Ground-Motion and isolator Characteristics. Earthquake Spectra 2006; 22 (4): 887-907.

Dicleli M. Supplemental Elastic Stiffness to Reduce Isolator Displacements for Seismic-Isolated Bridges in Near-Fault Zones. Engineering Structures 2007; 29, 763-775.

Dicleli M. Performance of Seismic-Isolated Bridges with and without Elastic-Gap Devices in Near-Fault Zones, Earthquake Engineering and Structural Dynamics 2008; 37 (6): 935-954.

Hatzigeorgiou GD, Damping Modification Factors for SDOF Systems Subjected to Near-Fault, Far-Fault and Artificial Earthquakes. Earthquake Engineering and Structural Dynamics 2010; 39 (11) 1239–1258.

Newmark NM, Hall WJ. Earthquake Spectra and Design EERI Monograph Series. Earth Engineering Research Institute: Oakland, CA, 1982.

Priestley MJN, Calvi GM and Kowalsky MJ. Displacement-Based Seismic Design of Structures. IUSS Press, Pavia, Italy, 2007

Lin YY, Chang KC. Study on Damping Reduction Factor for Buildings under Earthquake Ground Motions. Journal of Structural Engineering —ASCE 2003;129:206–14.

Cameron WI, Green RA. Damping Correction Factors for Horizontal Ground-Motion Response Spectra. Bulletin of the Seismological Society of America 2007; 97: 934–60.

Hubbard DT, Mavroeidis GP. Damping Coefficients for Near-Fault Ground Motion Response Spectra. Soil Dynamics and Earthquake Engineering 2011; 31: 401-417.

Pacific Earthquake Engineering Research Center. PEER Strong Motion Database. Available from: https://ngawest2.berkeley.edu/spectras/new. Last access: 2019/02/25.

Jacobsen LS, Ayre RS. Engineering Vibrations. New York: McGraw-Hill; 1958

Makris N, Black CJ. Dimensional Analysis of Rigid-Plastic and Elastoplastic Structures under Pulse Type Excitations. Journal of Engineering Mechanics, ASCE 2004;130(9):1006–18.

Makris N, Black CJ. Dimensional Analysis of Bilinear Oscillators under Pulse-Type Excitations. Journal of Engineering Mechanics, ASCE 2004; 130(9):1019–31.

Mestav SG, Askan GA, Caner A, Development of mean site-dependent response spectra for new bridge designs in Turkey. Structure and Infrastructure Engineering 2016; 13(8):1002–1012.

SAP 2000 V.15 Computers and Structures INC., Berkeley, CA, USA, 2015